Volume 17 | Number 4 | December 2014

IFSCC MAGAZINE

The Global Publication of the International Federation of Societies of Cosmetic Chemists

AFM Study of Hair Surface Deposition, Smoothness, and Mechanical Properties and Their Effects on Hair Shine and Conditioning

Chemical characterization of natural cosmetic ingredients: New insights on identification strategies

The Skin Firming “Red-volution”: Anti-cellulite Efficacy of a Papaver rhoeas Extract

Sunscreens – UV or Light Protection

Multicenter Study on the Effect of Various Test Parameters on the Curl Retention Results of Hairsprays

www.ifscc.org

Scientific Papers

AFM Study of Hair Surface Deposition, Smoothness, and Mechanical Properties and Their Effects on Hair Shine and Conditioning
Timothy Gao, Sam Zhu, Farahdia Edouard, Marni Dexter,, Jung-Mei Tien 3

Chemical characterization of natural cosmetic ingredients: New insights on identification strategies
Jane Hubert, Romain Reynaud, Jean-Marc Nuzillard, Sarah Öttl[c], Judith Rollinger[c], Jean-Hugues Renault 11

The Skin Firming "Red-volution": Anti-cellulite Efficacy of a Papaver rhoeas Extract
Thierry baldecchi, Lilia Heider, Marina Lefort, Christophe Carola, Claudia Cartigliani, Adirana Bonfigli, Frank Pflücker 19

Sunscreens – UV or Light Protection
J. Lademann, M.E. Darvin, H.-J. Weigmann, S. Schanzer, L. Zastrow, O. Doucet, H. Meffert, J. Krutmann, D. Kockott, T. Vergou, M.C. Meinke *23*

Multicenter Study on the Effect of Various Test Parameters on the Curl Retention Results of Hairsprays
U. Aßmus, S. Bielfeldt, H.-M., H. Hensen, P. Hössel, G. Lang, H. Leidreiter, A. Markowetz, V. Martin, B. Nöcker, M. Pfaffernoschke, E. Poppe, H. Schmidt-Lewerkühne, A. Schwan-Jonczyk, J. Wood, F.-J. Wortmann *29*

IFSCC Magazine:
Official scientific magazine of the International Federation of Societies of Cosmetic Chemists

Publications Chair:
Andrea Weber, Germany

Chair Science Committee:
Fujihiro Kanda, Japan

Chair Education Committee:
Miki Minaminu, Japan

Scientific Editor:
Lothar Motitschke, Germany

Language Editor:
Marcia Franzen-Hintze, Germany

Honorary Auditors:
Anne Hunt, France
Judy Beerling, United Kingdom

4 issues / year

ISSN# 1520-4561

IFSCC Office/Publisher's Office

IFSCC
Suite 109, Christchurch House
40 Upper George Street Luton, Beds LU1
2RS, UK Tel: +44-1582-72 66-61
Fax: +44-1582-40-52-17
lorna.weston@ifscc.org

Front Cover Design:
Fabian Mai
fabian.mai@sofw.com

Layout:
Andrea Weber
andrea.weber@babor.de

Important Information

From 2014 onwards we publish the contents of the IFSCC Magazine on the IFSCC Website:
www.ifscc.org

You will have to sign in to the Member Zone where you can then find the Scientific Papers of the IFSCC Magazine
Detail to be found on the Website

You will find the contents on the IFSCC Website as follows:

News from Member Societies:
News Page on Website

Awards:
Awards Pages on Website

Educational Programs:
Education Pages on Website

Scientific Papers:
Member Zone

IFSCC INTERNATIONAL FEDERATION OF SOCIETIES OF COSMETIC CHEMISTS

AFM Study of Hair Surface Deposition, Smoothness, and Mechanical Properties and Their Effects on Hair Shine and Conditioning

Timothy Gao, Sam Zhu, Farahdia Edouard, Marni Dexter, and Jung-Mei Tien
Croda Inc., 300-A, Columbus Circle, Edison, NJ, 08837, USA

Part of the work of this paper was presented at the 2012 and 2013 SCC Annual Scientific Conferences, New York City, USA, and 22nd IFSCC Conference 2013, Rio de Janeiro, Brazil.
Keywords: AFM, 3D imaging, hair conditioning, hair shine, hair surface smoothness

ABSTRACT

A new AFM 3D imaging technique was developed and applied to investigate correlations between consumer-perceivable hair shining, color vibrancy, and conditioning performance and nanoscale changes in hair surface roughness and mechanical properties before and after different cosmetic treatments. Changes in surface energy of hair fibers after different conditioner treatments were also detemined. Experimental results and subjective evaluations indicated that a thin oil or solid quaternary compound film is found on the hair surface after the respective hair shine spray or quaternary conditioner treatments. In addition, the deposited oil and quat film made the hair surface smoother and softer. The quat film also made the hair surface more hydrophobic and, subsequently, reduced the hair surface energy. As a result, hair shine spray-treated hair looked shinier and more color vibrant, and conditioner-treated hair tresses became easier to comb and felt smooth, soft, and sleek. The quat deposition and hair conditioning performance depended on the type of hair (damaged or virgin) and major ingredients contained in the applied conditioners.

AFM 3D imaging technology provided a very powerful tool to characterize hair surface morphological and mechanical properties. These nanoscale properties correlated well with instrumental measurements and consumer perceptions, such as hair shine, color vibrancy, hair feel, and hair conditioning.

INTRODUCTION

Hair shine is an important feature of hair appearance, and this attractive visual effect is a key consumer objective in the hair care market. Hair color strength/intensity is a very important attribute for colored hair. Previously, we developed methods for measurements of hair shine and surface smoothness by using a SAMBA system [1]. In 2010, we extended our study on colored hair and defined a new parameter, the Hair Color Vibrance Factor (HCVF) to describe comprehensive effects of hair shine and color strength (Chroma) [2]. Recently, we used advanced AFM 3-D imaging technique to study changes in hair surface integrity after different hair straightener treatments [3]. It is found that AFM is a very useful tool to study hair surface morphological properties: cuticle heights, cuticle angles, and surface roughness.

AFM has been widely used to study hair surface properties by Professor Bhushan and his group at Ohio State University [4]. In this review article, they present a comprehensive review of structural, mechanical and tribological properties of various hair and skin types as a function of ethnicity, damage, conditioning treatment, and various environments. But correlations between the nanoscale characterization of hair surface and consumer-perceivable performance have not yet been explored. In this paper we used the newly developed AFM technology of quantitative mechanical property mapping (PeakForce QNM) from Bruker [5] to investigate nanoscale changes in surface morphological and mechanical properties and correlate them with consumer-perceivable performance – hair shine, color vibrancy, and hair conditioning.

In order to have a better understanding of how hair surface morphology in nanoscale affects consumer-perceivable hair shine and color vibrancy, we first used a SAMBA system to measure the shine index, apparent cuticle angle (ACA), and HCVF of hair tresses before and after a hair shine spray treatment. We then used the AFM 3D imaging technique to determine nanoscale changes in the average cuticle height, average cuticle angle, and average surface roughness of hair fibers after the hair shine spray treatment relative to before. Subjective evaluations by panelists were also conducted. All experimental results helped us to establish multidimensional correlations among hair surface smoothness, hair shine/color vibrancy, and consumer perception.

Hair conditioning performance is a very important attribute of hair care products. Good hair conditioning products make hair easier to comb, feel moisture-rich, smooth, sleek and soft, and look shiny. In our previous research work on hair surface energy and conditioning[6], we found that the average surface energy of hair fibers treated with conditioners decreased and the hydrophobicity of the hair surface increased. The percentage changes in hair surface energy depend on the types of hair and major ingredients in the applied conditioner. These experimental results correlated well with the reduction in combing forces and salon evaluations after respective treatments. In this paper, we report our recent studies on surface film depositions of different quaternary conditioners on various types of hair. Different quat films exhibited different mechanical properties such as the elastic modulus, adhesion force, and deformation. Deposition of cationic quaternary conditioners showed a good correlation with the reduction in hair surface energy and improvement in hair conditioning performance.

EXPERIMENTAL

Materials

Virgin dark brown Caucasian hair and regular bleached hair were purchased from International Hair Importers and Products, Inc. (Glendale, NY).

A hair shine spray and two conditioners were prepared by the Application Group of

Croda Inc. and used to treat hair tresses for shine and combing force measurements, surface energy measurements, and AFM imaging. The hair shine spray contained 55% Cyclomethicone and 45% PPG-3 Benzyl Ether Ethylhexanoate. Conditioner-A (Q-91 Conditioner) contained 2.14% of Quaternium-91 (and) Cetrimonium Methosulfate (and) Cetearyl Alcohol, 3.86% of Cetearyl Alcohol, 0.10% of Methylisothiazolinone, the rest was balanced with DI-water. Conditioner-B (BTMS Conditioner) contained 3.00% of Behentrimonium Methosulfate (and) Cetyl Alcohol (and) Butylene Glycol, 3.00% of Cetearyl Alcohol, 0.10% of Methylisothiazolinone, and the rest was made up with DI-water. Both the Q-91 and BTMS conditioners had the same amount of active quaternary compounds, 1.5%.

The hair spray was applied to both sides of each tested hair tress at three positions - top, middle, and bottom - and the tresses combed through to distribute the spray evenly. 2 g of the conditioner were left on each hair tress for 3 minutes and then the tress rinsed under 40 °C tap water (flow rate 800 ml/min) for one minute. The treated tress was dried at room temperature overnight.

Instruments and test methods:

A Krüss K100 automatic Tensiometer from Krüss, Hamburg, Germany was used for measurements of dynamic advancing contact angles and surface energy of hair fibers before and after the respective conditioner treatments [6].

An AFM (Dimension Icon System from Bruker AXS, Karlsruhe, Germany) equipped with a peak force quantitative nanoscale mapping (QNM) mode was used to capture 3D images of hair fibers and the NanoScope Analysis computer software from Bruker for data analysis of hair surface morphological and mechanical properties [5]. All measurements were done at a constant temperature (22 °C) and 60% relative humidity. An RFESP probe (1-10 Ohm-cm phosphorus (n) doped Si) from Bruker was used in the PeakForce QNM Tapping mode.

A DiaStron Miniaturer Tensile Tester MTT-175 from Dia-Stron Limited, Hampshire, UK was used to determine wet and dry combing forces of hair tresses before and after the respective conditioner treatments. The dry combing force measurements were performed in an environmentally-controlled chamber at 60% RH and 22 °C.

A SAMBA Hair Color Imaging System from Bossa Nova Technologies, Venice, CA was used for measurements of the hair luster (L*), chroma (C), overlapping coefficient (Oc), and apparent cuticle angle (ACA) of hair samples before and after the hair spray treatments. Their HCVF values were calculated [2].

RESULTS AND DISCUSSION

Enhancement of hair shine and hair color vibrancy

AFM 3D imaging analysis of hair smoothness, surface roughness, cuticle height, and cuticle angle

We have developed a technology to obtain AFM images of the same section of a hair fiber before and after a cosmetic treatment. **Figures 1 and 2** are typical AFM 3D images of the same section of a virgin dark hair fiber before and after the hair shine spray treatment. **Figures 3 and 4** are the corresponding "section analysis" profiles. A total of 10 hair fibers were used for these measurements; nine "section lines" per image were used to calculate the average values of the cuticle angle, cuticle height and surface roughness for each image. Average percentage changes in the cuticle height, cuticle angle, and surface roughness of a hair fiber after the hair-spray treatment relative to before were calculated. Then the average changes in these parameters of 10 hair fibers were calculated and listed in Table I. A t-test statistical analysis was performed for each parameter determined.

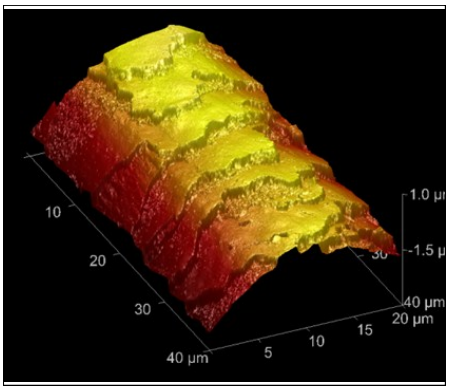

Figure 1: AFM image of a section of hair fiber before treatment

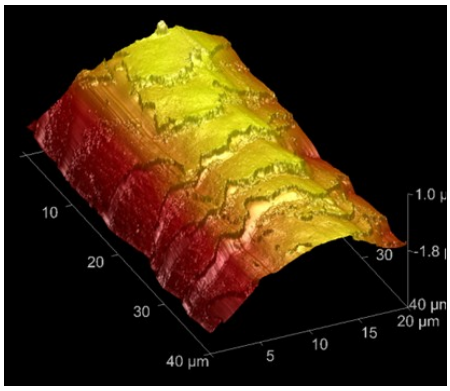

Figure 2: AFM image of the same section of hair fiber after treatment

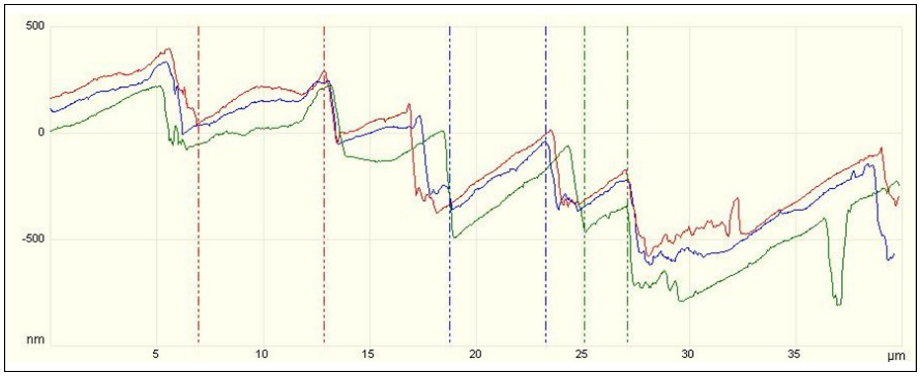

Figure 3: Section analysis profile of Image 1

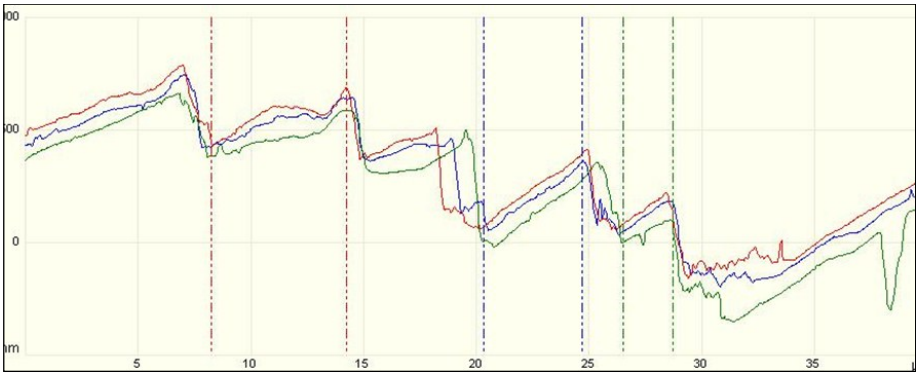

Figure 4: Section analysis profile of Image 2

Table I Results of AFM Section Analysis

Average Cuticle Height (nm)			Average Cuticle Angle (°)			Average Surface Roughness (nm)		
Before	After	Change (%)	Before	After	Change (%)	Before	After	Change (%)
243	205	-15.6±2.5	3.5	2.8	-20	265	250	-5.7

From **Figure 2**, it can be seen that edges/ gaps of cuticles were partially filled with deposited oil films. The experimental results in **Table I** show that deposited oil films reduced the average cuticle height by 15.6% and decreased the cuticle angle by 20%. The average surface roughness was reduced about 15 nm (5.7%). It is apparent that the hair surface was smoother after the treatment. Statistical analysis of these values indicates that these differences are statistically significant with 95% confidence.

The surface deformation images of a section of hair fiber before and after treatment with hair spray are presented in **Figures 5 and 6**, respectively. It can be seen that upon application of a nano-Newton force by the AFM probe, the oil film (as a soft material) showed dramatically higher deformability than the hair cuticle (as a hard material). Thus, hair spray oil can be spotted on hair surface by surface deformation mapping. The actual deformation reading can be used to estimate oil film thickness. It was determined that the sprayed oil formed an approximately ~ 10 nm thick liquid film on the hair fiber surface. The liquid gradually spread and accumulated in cracks and on cuticle edges.

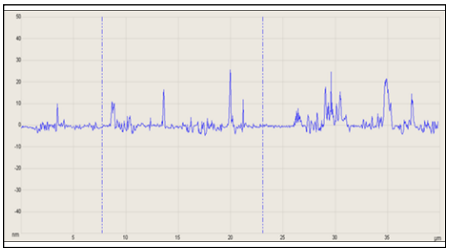

Figure 5:Surface deformation of an untreated section of hair fiber

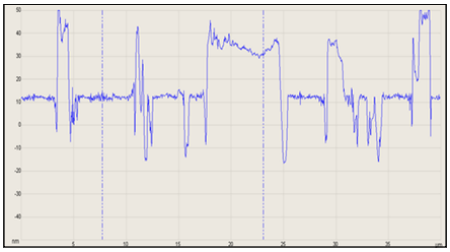

Figure 6: Surface deformation of the same section of hair fiber treated with

AMBA measurements

Average values of hair shine (L), HCVF, and ACA of 5 dark brown or bleached hair tresses before and after the hair shine-spray treatment were determined using a SAMBA system. Three readings were taken on each side of every tested hair tress, two tress orientations (root to tip and tip to root) were measured, and a total of 12 values of each parameter were averaged for each tress. Percentage changes in each parameter of every tested tress were calculated and the average changes in 5 hair tresses were calculated. The data are summarized in **Table II**.

It can be seen that the hair shine spray improved the hair shine value on virgin and bleached hair on average by 12% and 44%, respectively, and reduced the apparent cuticle angle by 8.1% and 21.9%, respectively. The HCVF increased 18.9% and 48.6%, respectively.

Statistical analysis of these experimental data showed the differences after the hair spray treatment relative to before to be significant with 95% confidence.

Subjective evaluations by panelists

Subjective evaluations of hair shine and color vibrancy were conducted by 25 panelists. 96% of the panelists confirmed that the spray-treated hair tresses were shinier with more vibrant color. From the above experimental results and these subjective evaluations, it is apparent that the nanoscale measurements provide a good indication of consumer-perceivable performance for hair shine and color vibrancy.

Improvement in hair conditioning performance

AFM Study of morphological and mechanical properties of the hair surface

Typical AFM 3D images of virgin dark hair fibers before and after Q-91 conditioner treatment are presented in **Figures 7-1 and 7-2**, respectively. Although we used the exact same section of hair fiber for AFM imaging before and after conditioning, the images are slightly different due to the scanning process at different times and possible environmental changes.

Figures 7-3 and 7-4 depict the surface roughness before and after the conditioner treatment. Ten hair fibers were used for image analysis and nine profile lines were taken on each hair image. A total of 90 values were determined for the measured parameter. It was found that the average maximum roughness of the treated hair surface is only 1.2 mm and that of the untreated surface 2.0 mm, indicating that the treated hair surface was much smoother.

The foundation of material property mapping with PeakForce QNM is the ability of the system to acquire and analyze the individual force curves from each tap that occurs during the imaging process. To separate the contributions from different material properties such as adhesion, modulus, dissipation, and deformation, it is necessary to measure the instantaneous force on the tip rather than a time-average of the force or dissipation over time, as is done in Tapping-Mode PhaseImaging™. Peak Force QNM mode AFM is used to obtain high resolution of the mechanical properties of a scanned surface, including the elastic modulus, deformation, adhesion force, and dissipation of hair samples [5]. **Figures 8-1 and 8-2** are typical elastic modulus images of a virgin hair fiber before and after the Q-91 conditioner treatment, respectively. "Particle Analysis" software was used to generate images of the surface based on the difference in the elastic modulus. **Figures 8-3 and 8-4** present the surface depositions for untreated and treated hair surface. The untreated hair

Hair sample	Shine value (L*)			Hair color vibrance factor (HCVF)			Apparent cuticle angle (°)		
	Before	After	Change (%)	Before	After	Change (%)	Before	After	Change (%)
Dark brown	36.0	40.3	12.0±1.8	65.2	77.5	18.9	1.90	1.75	-8.1±1.2
Bleached	5.0	7.2	44.0±8.2	7.0	10.4	48.6	1.60	1.25	-21.9±2.6

Table II Results of SAMBA Measurements

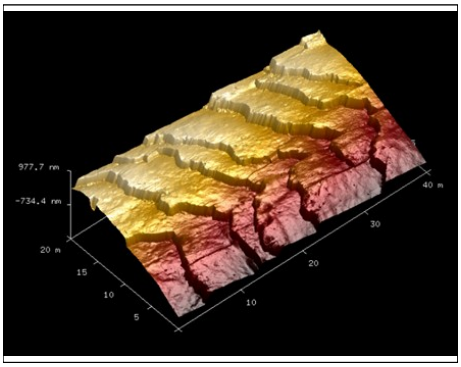

Figure 7-1:
AFM 3D image before conditioner treatment

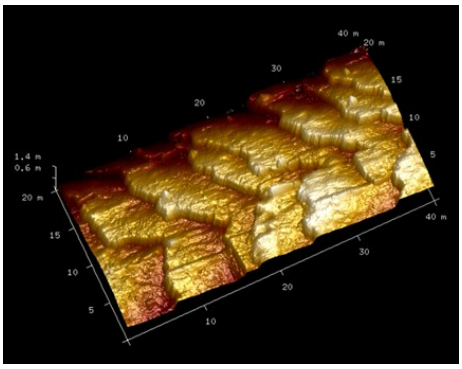

Figure 7-2:
AFM 3D image after conditioner treatment

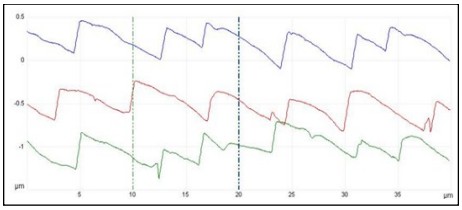

Figure 7-3: Surface roughness before conditioner treatment

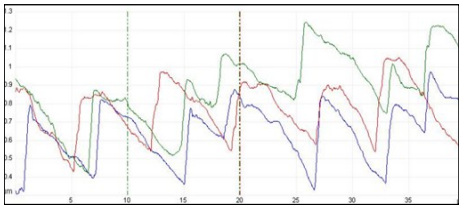

Figure 7-4: Surface roughness after conditioner treatment

surface showed a higher elastic modulus (average 2.23 GPa) and almost no deposition on the surface. The Q-91 conditioner-treated hair surface showed a lower average elastic modulus (1.04 GPa) and accordingly a large deposition area on the surface (blue color).

The second important mechanical property of hair surface is the adhesion force, which is a measure of interactions (attractive force) between the AFM probe tip and the hair surface. If either the hair surface or the probe surface is hydrophilic, a capillary meniscus will typically form, leading to a higher adhesion force (surface energy). **Figures 9-1** and 9-2 show the adhesion force images of untreated and Q-91 conditioner-treated virgin hair samples, respectively. The treated hair surface exhibited a lower average adhesion force (1379 nN) and the untreated surface a higher adhesion force (1883 nN). This indicated that the treated hair surface became more hydrophobic and had a lower surface energy.

Another important surface mechanical property is the maximum deformation, defined as the penetration of the tip into the surface at the peak force. The measured deformation includes both elastic and plastic contributions. This property can also be converted to the surface hardness. **Figures 10-1 and 10-2** represent deformation images of untreated and treated virgin hair samples. The darker color indicated smaller deformation and lighter color represents larger deformation. The calculated results showed that the untreated hair surface had a maximum deformation of 0.54 nm, while that of the treated hair sample was 2.24 nm. It is clear that the deposited conditioner film made the hair surface softer.

To determine the deposition of different quats on different hair surfaces, Q-91 conditioner and BTMS conditioner were each applied to virgin dark brown hair and bleached hair, respectively. Ten hair fibers each of virgin hair and bleached hair were used for measurement and AFM imaging. Three adjacent sections of each fiber were used for the control (untreated), Q-91 condi-

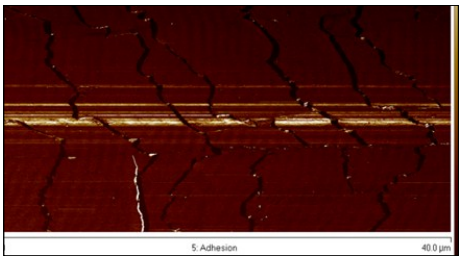

Figure 9-1: Adhesion force before conditioner treatment

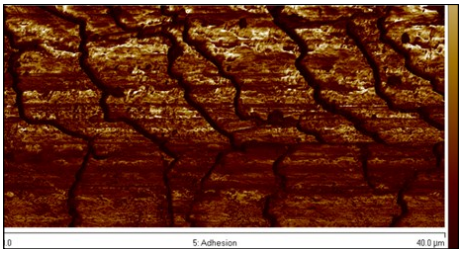

Figure 9-2: Adhesion force after conditioner treatment

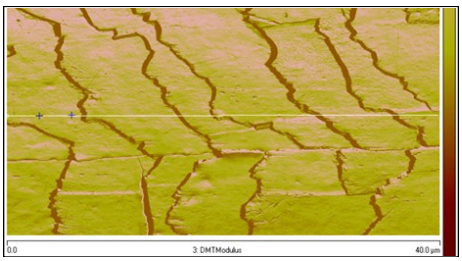

Figure 8-1: Elastic modulus before conditioner treatment

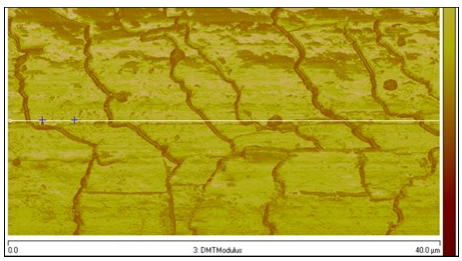

Figure 8-2: Elastic modulus after conditioner treatment

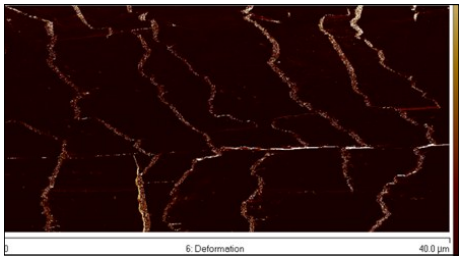

Figure 10-1: Deformation before conditioner treatment

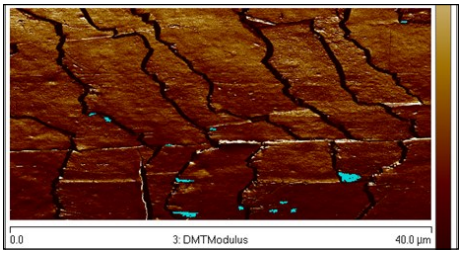

Figure 8-3: Particles before conditioner treatment

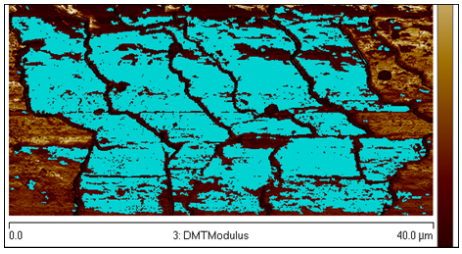

Figure 8-4: Particles after conditioner treatment

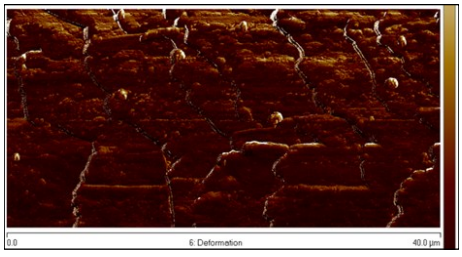

Figure 10-2: Deformation after conditioner treatment

Hair sample	Roughness (nm)		Adhesion (nN)		Deformation (nm)		Elastic modulus (Gpa)	
	Virgin	Bleached	Virgin	Bleached	Virgin	Bleached	Virgin	Bleached
Control	642±92	595±105	1030±148	1885±285	65.6±10.1	58.6±8.8	1.28±0.18	2.23± 0.35
Q-91 treated	190±27	476±72	717±105	1240±192	80.3±11.5	93.4±14.0	0.70±0.11	0.74±0.11
BTMS treated	223±31	374±55	833±123	985±151	75.3±11.5	82.3±12.5	0.81±0.12	0.84±0.13

Table III Surface Roughness and Mechanical Properties of Hair Surface

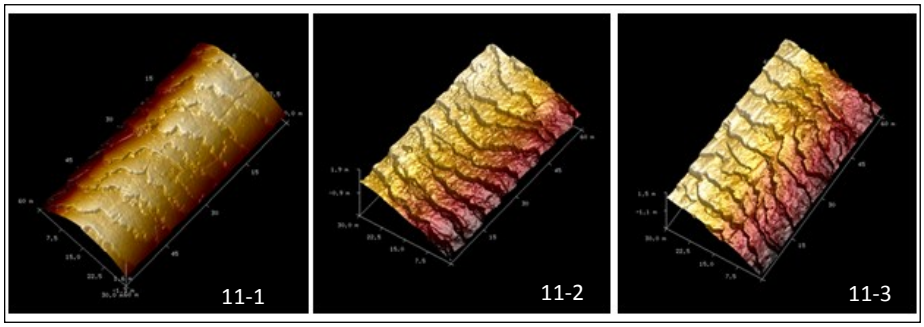

Figure 11-1: AFM 3D image of an untreated virgin hair fiber
Figure 11-2: AFM 3D image of a virgin hair fiber treated with Q-91
Figure 11-3: AFM 3D image of a virgin hair fiber treated with BTMS

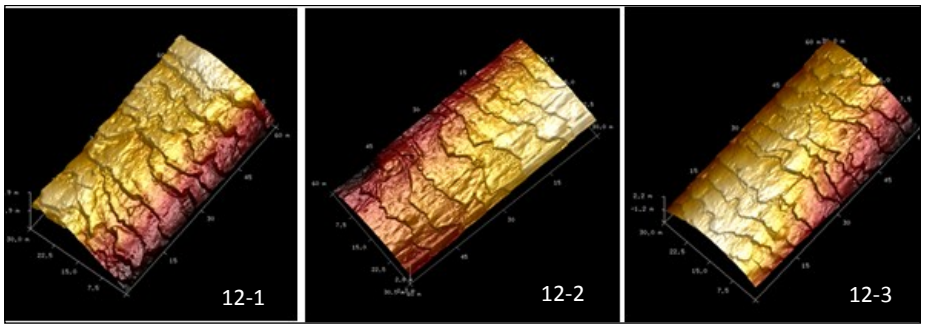

Figure 12-1: AFM 3D image of an untreated bleached hair fiber
Figure 12-2: AFM 3D image of bleached hair fiber treated with Q-91
Figure 12-3: AFM 3D image of a bleached hair fiber treated with BTMS

tioner treatment and BTMS conditioner treatment. The average mechanical properties of hair samples (sections) before and after a specific conditioner treatment were calculated using 10 fibers (sections). Typical AFM 3-D images of different hair samples with different conditioner treatments are presented in **Figures 11 and 12**. The average surface roughness and mechanical properties determined for all these hair samples are summarized in **Table III**.

The results in **Table III** show that both Q-91 and BTMS were deposited on the virgin dark brown hair and as well as on bleached hair surface. Moreover, the deposited quat films reduced hair roughness, made the hair surface more hydrophobic (lower adhesion force and surface energy), and less elastic (higher deformation). The reduction in hair surface roughness and adhesion force on virgin hair was greater with Q-91 , but on bleached hair the reduction was greater with BTMS. This can be attributed to their different molecular structure and interactions with different hair surfaces. BTMS is a cationic surfactant having one single C22 hydrocarbon chain and a positive-charged quaternary head. Q-91 is di-behenyl imidazolinium methasulfate. Its positive charge is distributed over a resonance structure of three atoms (two nitrogen and one carbon), which gives it a weaker charge density than BTMS. Therefore BTMS interacts more strongly with the damaged, negatively charged surface of bleached hair. On the other hand, Q-91 showed good deposition on undamaged virgin hair surface. Since the deposited Q-91 layer has a double C22 hydrocarbon chain towards the outside of the hair surface, it probably showed higher deformation and a smaller elastic modulus than a single chain of the BTMS layer.

Change in surface energy after quat deposition

Dynamic advancing contact angles of hair fibers before and after the respective conditioner treatments were determined in deionized water, Di-iodomethane, in benzyl alcohol, respectively. These values were used to calculate the surface energy of each single hair fiber [6]. The percentage changes measured for 30 single fibers with the same treatment were averaged to obtain the average changes in surface energy of hair fibers after the respective conditioner treatments. The results are summarized in **Tables IV and** V and presented in **Figure 13**.

The surface energy of Q-91conditioner treated bleached and virgin hair was reduced by 29.06% and 31.77%, respectively, which indicated that the Q-91 conditioner produced a similar reduction in surface energy on both hair types. These results corresponded well with results on percentage changes in the combing forces of Q-91 conditioner treated bleached and virgin hairs. The average surface energy of bleached hair and virgin hair treated with the BTMS conditioner decreased by 33.72% and 27.64%, respectively. It is apparent that the BTMS conditioner showed better conditioning performance on the bleached hair with a damaged hair surface. This is consistent with the combing force reduction results.

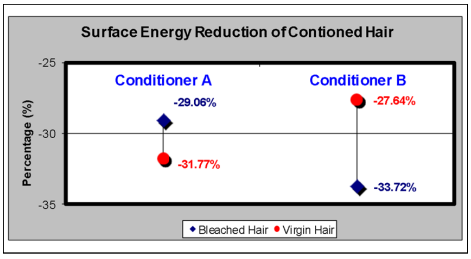

Figure 13: Reduction in surface energy after different conditioner treatments

	Q-91 Conditioner			BTMS Conditioner		
Surface energy, mJ/m²	Original	After treatment	Change (%)	Original	After treatment	Change (%)
Polar	2.18± 0.32	1.79±0.28	-18.0±2.6	1.87± 0.28	1.79±0.27	-4.4±0.6
Dispersive	27.65± 4.02	19.38±2.81	-29.9±4.4	25.03± 3.71	16.04±2.40	-35.9±4.2
Total	29.83± 4.32	21.17±3.21	-29.0±3.7	26.90± 4.01	17.83±2.63	-33.7±5.0

Table IV Change in Surface Energy of Conditioner-A/B Treated Bleached Hair

	Q-91 Conditioner			BTMS Conditioner		
Surface energy, mJ/m²	Original	After treatment	Change, %	Original	After treatment	Change, %
Polar	2.48± 3.70	1.77±0.25	-28.7±3.2	0.64± 0.10	0.45± 0.07	-28.9±4.5
Dispersive	16.41± 2.42	11.12±1.65	-32.2±4.8	17.83± 2.52	12.91± 1.90	-27.6±4.0
Total	18.89± 2.74	12.89±1.80	-31.2±4.5	18.47± 2.73	13.36± 2.01	-27.6±4.2

Table V Change in Surface Energy of Conditioner-A/B Treated Virgin Hair

Reduction in combing forces of hair tresses

The surface energy reflects a microscale surface property of a hair fiber; experimental data were derived from each single hair fiber. The wet combing force is a macroscale property of a hair tress (assembly); it is determined by interactions between hair fibers (and water) as well as between fibers and comb teeth. It is expected that the lower the surface energy is, the weaker the interactions between hair fibers and the smaller the wet/dry combing forces between the comb teeth and hair fibers should be.

To study the correlations between the decrease in surface energy and reduction in combing forces, bleached and virgin hair tresses were treated separately with Q-91 conditioner and BTMS conditioner and percentage changes in the wet combing forces of hair tresses after different conditioner treatments were calculated. **Figures 14-1 and 14-2** show the correlations between the change in surface energy and reduction in wet combing forces of treated hair tresses.

It can be seen that the Q-91 conditioner reduced the surface energy of both bleached and virgin hair fibers to similar levels and showed comparable conditioning performance on both hair types. The BTMS conditioner produced a larger reduction in surface energy on bleached hair fibers and demonstrated better conditioning performance on bleached hair. The reduction in the surface energy of hair fibers corresponds well to the decrease in wet combing forces of treated hair tresses

Salon – consumer perceivable evaluations

Forty panelists (20 persons with damaged (dyed) hair and 20 persons with non chemical-treated (virgin) hair) participated in the study. A half head test design was used for the study: Q-91 conditioner and BTMS conditioner were applied to the panelists' wet clean hair on the left and right side, respectively. Then the conditioners were rinsed out and the hair was blow-dried. The hair was evaluated for a total of 10 wet and dry attributes (detangling, wet combing, wet feel, dry combing, dry feel, dry sheen, bounce/body, softness, volume and spreadability) on a scale of 1 to 10 (10 is the best). The average scores were calculated for the 10 attributes.

The results of the salon evaluations indicated that BTMS demonstrated better 'wet feel' and 'volume' on colored hair than the Q-91 conditioner; Q-91 showed better 'dry feel' and 'softness' on virgin than the BTMS conditioner. In general, there were no significant differences in conditioning performance observed between the Q-91 conditioner and BTMS conditioner on either colored or virgin hair.

CONCLUSIONS

The AFM PeakForce QNM 3-D imaging technique was used successfully to study hair surface smoothness and quat deposition. Deposited thin films of quats on hair surfaces were validated by images and changes in surface morphological and mechanical properties.

Nano-characterization of hair smoothness provided a good indication of hair shine: the smoother the hair surface, the shiner the hair and higher the Hair Color Vibrance Factor. Objective measurements of hair shine

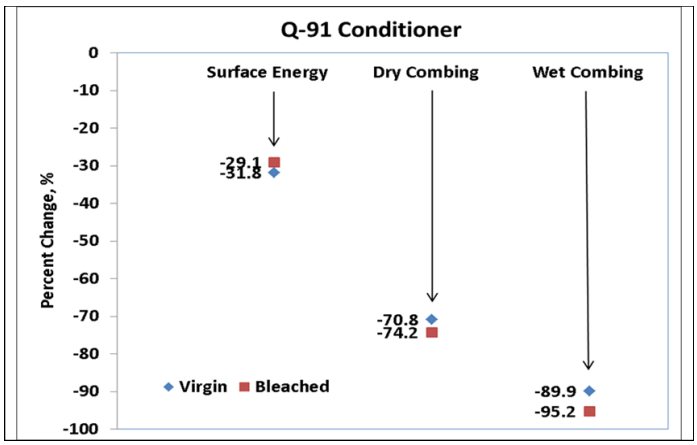

Figure 14-1: Correlation between change in surface energy and reduction in wet combing forces for Q-91 conditioner-treated hair tresses

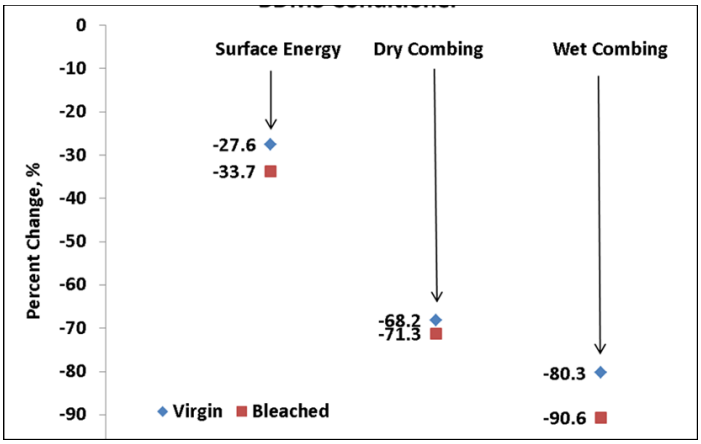

Figure 14-2: Correlation between change in surface energy and reduction in wet combing forces for BTMS conditioner-treated hair tresses

and HCVF demonstrated good agreement with consumer-perceivable performance.

Quat deposition depends on both the hair surface condition (damaged or undamaged) and the molecular structure of the conditioner used. The BTMS conditioner with a higher molecular charge density showed better deposition on the surface of damaged hair than did the Q-91 conditioner, which has a delocalized charge distribution in the molecule [7]. The deposited quat films made hair surfaces smoother, more hydrophobic, and softer. They also reduced the surface energy and made the hair easier to comb. The reductions in surface energy of treated hair fibers correspond well with the decreases in wet combing forces of treated hair tresses.

Results of consumer perceivable evaluations showed a comparable conditioning performance of both conditioners on virgin and colored hair.

REFERENCES

[1]. Gao, T., Pereira, A., and Zhu, S., "Study of Hair Shine and Hair Surface Smoothness", J. Cosmet. Sci., 60(2), 2009, 187 – 197.

[2]. Gao, T., Landa, P., Tillou, R., and Gallagher, G., "Hair Color Vibrance Factor to Characterize Shine and Color Intensity", C&T magazine, 127 (1), 2012, 48-56.

[3]. Gao, T., Moses, C., Li, Z., Tien, J.M., He, Y.X., and Landa, P., "A New Hair Straightening System Showing High Performance and Low Damage", J. Cosmet. Sci., 63(1), 2012, 64 – 65.

[4]. Bhushan, S., "Nanoscale characterization of human hair and hair conditioners", Progress in Material Science, 53, 2008, 585 -710.

[5]. AFM Operation Manual, "Quantitative Mechanical Property Mapping at the Nanoscale with PeakForce QNM", Bruker Corporation.

[6]. Gao, T., He, Y.X., and Landa, P., "Study of Hair Surface Energy and Conditioning", J. Cosmetic. Sci., 62(2), 2011, 127-137 .

[7]. Gao, T., Bedell, A., Tien, J-M., Pereira, A., Obukowwho P., and Comber, R., "Quaternium-91: a new multifunctional hair conditioning ingredient", C&T Magazine, Vol. 118(5), 2003, 47-56.

Corresponding author
email: timothy.gao@croda.com

IFSCC INTERNATIONAL FEDERATION OF SOCIETIES OF COSMETIC CHEMISTS

Chemical characterization of natural cosmetic ingredients: New insights on identification strategies

Jane Hubert[a], Romain Reynaud[b], Jean-Marc Nuzillard[a], Sarah Öttl[c], Judith Rollinger[c], Jean-Hugues Renault[a]

[a]Institut de Chimie Moléculaire de Reims (ICMR, UMR CNRS 7312), SFR CAP'SANTE, Université de Reims Champagne-Ardenne, France - [b]Soliance, Pomacle, France - [c]Institute of Pharmacy/Pharmacognosy, Center for Molecular Biosciences University of Innsbruck, Austria

This publication was presented as a podium presentation at the 28. IFSCC Congress, October 27-30, 2013, Paris, France.

Keywords: natural cosmetic ingredients, chemical profiling, dereplication

ABSTRACT

Natural ingredients from plants, marine or microbial organisms are a precious source of biologically active metabolites for the development of new cosmetics. However, the chemical complexity of these extracts still requires time-consuming multi-step separation and purification procedures to determine their chemical composition. New approaches for the direct analysis of metabolites within mixtures are currently the focus of intense research efforts, not only to save purification time and burden, but also to assess the potential synergistic effects between compounds. This document presents an overview of modern strategies which are currently used for the chemical characterization of natural mixtures and promise significant achievements in the cosmetics area. In particular a recently developed dereplication method is described which combines chromatographic, spectroscopic and data mining tools for the analysis of natural metabolite mixtures without purification of each individual substance. This approach was designed for an early application in cosmetics when the chemical characterization of natural active ingredients is subjected to increasing regulatory constraints. Its principle consists in rapidly generating a series of simplified fractions from a crude natural extract by centrifugal partition extraction, with each fraction subsequently analyzed by ^{13}C NMR. After automatic collection and binning of all ^{13}C NMR signals across the spectra of the fraction series, the resulting data set is subjected to hierarchical clustering analysis for pattern recognition. Strong signal correlations caused by the same structure in different fractions are directly visualized as clusters and subsequently assigned to a molecular structure using a natural metabolite database. Using two real-life examples we show that this approach presents a significant breakthrough for the rapid characterization of natural active ingredients.

INTRODUCTION

Despite the difficult economic context in many occidental countries, the cosmetic industry currently remains a thriving sector, with predominant markets in Western Europe, North America and the Asia Pacific [1]. All companies constantly invest in research efforts for the development of new active and innovative ingredients, originally designed formulations, as well as reliable testing models. These steps are crucial because they demonstrate the originality, effectiveness and safety of the final products and allow a competing group to differentiate itself from the others in order to fulfill profitability objectives.

A wide diversity of natural extracts from microbial, plant or marine sources are appearing on the market at an exponential rate because natural species are able to produce unique secondary metabolites covering numerous chemical classes and exhibiting distinct physicochemical and biological properties. For instance a range of natural polysaccharides, such as β-glucans from yeast, bacteria, seaweeds or cereals, chitosan from the exoskeleton of crustaceans and levans from plants or microorganisms, are currently used in moisturizing creams for their emollient, filmogenic, and even anti-inflammatory properties [2-4]. Other natural metabolites including fatty acids, amino acids and protein hydrolysates are also promising candidates to improve skin elasticity [5], not to mention phenolic compounds, which are well-recognized for their keratolytic, purifying and antioxidant properties in addition to their astringent, anti-inflammatory and antimicrobial activities [6, 7].

However, the increasing use of natural ingredients in the cosmetic industry faces to several major issues due to their complex chemical composition. Firstly, the characterization of metabolite mixtures in natural extracts remains difficult to achieve, reference substances are most of the time unavailable for analytical comparison and biological data regarding their mechanism(s) of action are scarce [8]. Secondly, some constituents of natural ingredients may exhibit damaging properties, most often skin sensitization, eye irritation, genotoxicity, mutagenicity or UV-induced toxic effects [9]. Consequently, one of the key steps during the development of a cosmetic formulation besides acquiring a thorough knowledge about all metabolites is to guarantee their safety and time stability.

In this context, strict regulatory guidelines for the marketing authorization of cosmetics are gradually emerging together with the recent directives around the Registration, Evaluation, Authorization and Restriction of Chemicals (REACH) program, focused on environmental and health impacts of cosmetic product manufacturing [10]. Of course, in the case of natural extracts made of mixtures of metabolites, which may or may not act in synergy and some of which being potentially problematic from the safety point of view, all these constraints imply that the metabolite profile of natural ingredients must be fully characterized or at least perfectly controlled through standardization. Finally, it should be mentioned that the better the chemical profile of a natural ingredient is known, the more the industry that commercializes this ingredient brings added value to the final product and meets customer's expectations.

In practical terms, fully characterizing a natural ingredient in a reasonable amount of time presently remains a very hard task. Even though modern analytical and purification techniques are routinely available in most academic laboratories, considerable work taking several days or even several weeks or years is still necessary to systematically isolate individual constituents from crude mixtures and subsequently elucidate their molecular structure. In addition to be time-consuming, such a classical approach requires abundant human and technical resources and is thus economically unrealistic for the cosmetic industry.

As all scientists involved in natural product research (Agriculture, Nutrition, Health… …) share the same concerns regarding the chemical characterization of natural extracts, great investments have been made over the last years to develop more efficient fractionation, purification and analytical methods, as well as their combination with bioinformatics tools or inclusion in more integrative strategies.

This article provides an overview of the recent strategies for the chemical characterization of natural mixtures that are interesting for the development of cosmetic ingredients. In particular, a recently developed ^{13}C NMR-based dereplication strategy combining chromatographic, spectroscopic and data mining tools will be described and illustrated by two real-life examples of natural cosmetic ingredients.

STRATEGIES FOR CHEMICAL CHARACTERIZATION OF NATURAL MIXTURES

Metabolite profiling

Procedures known as "**metabolite profiling**" may help to meet some of the objectives, even though the complete chemical characterization of natural cosmetic ingredients remains a difficult task. Metabolite profiling is defined as the systematic identification and quantification of a range of compounds. Depending on the final purpose and the analytical technique(s) available, it can be performed either as a "**fingerprint analysis**" where all detected metabolites are not necessarily identified or as a "**targeted screening**" where a predefined number of compounds or a particular chemical class of compounds is covered (**Figure 1**).

Fingerprint analyses are currently very common non-targeted approaches to assess the quality of natural ingredients that must be checked for authentication, contamination, identification of the active substances or safety validation. These procedures are based on the fact that each natural extract, although highly complex, contains secondary metabolites which are specific to the species under study. During analytical data capture, the set of signals corresponding to these specific metabolites becomes a chemical fingerprint and the most characteristic signals can be selected as "chemical markers". Of course, variability of their content in natural raw materials is inevitable due to inherent factors such as genotypic variability or growing conditions like climate and soil type [11]. By tracking chemical markers over different steps of the manufacturing process a fingerprint analysis can serve to control this variability and minimize the potential composition heterogeneity of the final ingredient from one batch to another. This process forms an integral part of the standardization of cosmetic ingredients, a major task which is absolutely necessary to adjust the concentration of the active substances and ensure a reproducible quality of the final products.

It should also be noted that the chemical markers of a cosmetic ingredient theoretically correspond to the biologically active substances. However, sometimes the amounts of markers are not consistent with the biological activity [12]. This can happen when a marker is selected only because it is among the major constituents of the natural extract and thus more easily quantified. Ideally, both chemical and biological markers should be rigorously selected and clearly differentiated to rationally achieve the standardization of natural active ingredients.

Targeted screening of natural extracts consists in analyzing a predefined group of known metabolites. In the context of cosmetics such an approach can be used to determine the presence of a particular chemical class in natural ingredients, as was done recently by ^{1}H NMR to screen fatty acids in microalgae for functional health product development [13]. A targeted screening enables also assessment of the toxicological risk arising from the presence of particular molecular structures in an ingredient. For instance, the screening of coumarin derivatives, which are widely employed as fragrances in cosmetic products, has recently proven to be important due to high skin absorption levels and possible irritation disorders following topical applications of particular coumarin-derived substances [14].

Metabolite profiling analyses in the cosmetic industry are most frequently performed by thin layer chromatography (TLC) or its upgraded version, high performance thin layer chromatography (HPTLC), because of their quickness, moderate cost, and automation capabilities [15]. Infrared (IR) spectroscopy can also be used to rapidly assess the presence of particular functional groups in samples. This technique requires no extraction, is non-destructive and rapid, and is thus highly suited for the analysis of a high number of natural samples, for instance, to compare different batches of raw materials, assess the presence of contaminant or predict the concentration of particular classes of constituents [16].

Other more sophisticated analytical systems such as high performance liquid chromatography (HPLC) or gas chromatography (GC) hyphenated to ultraviolet (UV) detection, mass spectrometry (MS) or nuclear magnetic resonance (NMR) may also be employed to perform metabolite profiling analyses [17]. They can be used just to check the identity, quality and stability of active ingredients by fingerprinting or chemical marker tracking but also offer the possibility to elucidate the structure and/or quantitatively measure the content of phytochemical constituents in natural ingredients. Among the most recently developed post-genomic technologies, metabolomics has also emerged as a valuable tool for the metabolic profiling of natural extracts. Such an approach aims to qualitatively or quantitatively analyze the whole set of metabolites present in biological systems by com-

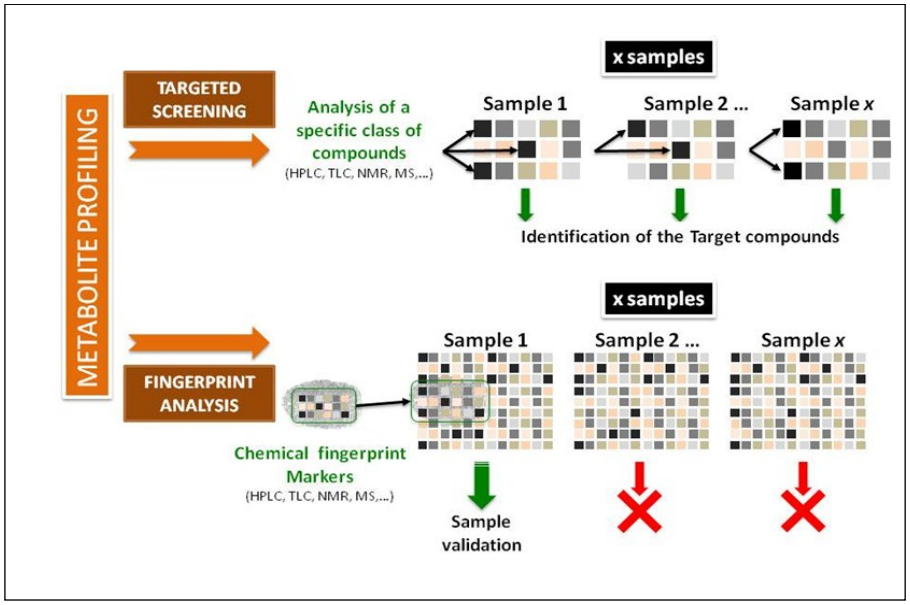

Figure 1 Schematic workflow of metabolite profiling approaches

bining state-of-the-art spectroscopic instruments, bioinformatics tools and metabolite databases [18]. In the field of natural products, metabolomics has been primarily used to control the quality of herbal medicines, assess the toxicological profile of natural substances, evaluate the chemical differences between plant species or determine correlations between bioactivity and composition [18-20]. Its application to cosmetics might thus be significant for assessing the chemical profile of natural active ingredients.

Bioactivity-Guided Natural Product Screening

Another commonly used strategy for the chemical characterization of natural extracts refers to the so-called "**bioactivity-guided fractionation**" procedures in which biological assays are performed to target the isolation of bioactive constituents (**Figure 2**). They initially were developed to avoid wasting time and resources considering inactive, arbitrarily implied "uninteresting" compounds, and thus to focus only on the fractions or metabolites with a selected biological activity [21].

Once active fractions have been found by biological evaluation, classical separation and analytical techniques are then applied to isolate and structurally elucidate the individual active substances. Use of such procedures has become very common for the investigation of natural ingredients, and a range of chemical, enzymatic and *in vitro* biological tests (e.g. antioxidant, antimicrobial, antifungal, anti-inflammatory) are today available [22]. Mostly based on UV absorbance measurements, these assays are generally fast, easy to operate, sensitive, and do not require large quantities of materials. Most of them can be fully or partly automated. TLC-based bioautography has been also reported as a useful and cost-effective technique for a preliminary biological screening of natural extracts [23]. Of course *in vivo* models would result in more consistent data regarding biological activities of natural extracts but their use is limited by economic and ethical concerns, particularly the use of animal models or tissues, which is severely restricted in the field of cosmetics.

It should also be noted that bioactivity-guided fractionation procedures are based on the theory that the activity shown by a mixture of metabolites results directly from the sum of activities of the individual metabolites. However, it is becoming evident that the biological effects of a natural extract most likely result from a multi-component synergism [24, 25]. As a consequence, the major drawback of bioactivity-guided fractionation procedures arises from the frequent loss of activity after metabolite separation. Other limitations have been reported for bioactivity -guided fractionation procedures including the frequent rediscovery of already known compounds, poor solubility of the separated constituents in the bioassay medium, difficulty in separating very polar active fractions and irrelevance of most *in vitro* bioassays to *in vivo* or clinical conditions regarding either the efficacy or bioavailability of the samples under examination [26]. In addition, nothing is known about the active constituents of a large number of natural extracts. Potentially interesting compounds may also be missed just because they are not active in the selected bioassays.

Dereplication strategies in natural product research

The two previous sections provide evidence that metabolite profiling and bioactivity-guided fractionation procedures may be useful strategies to partly address the issues related to the chemical characterization of natural ingredients. These approaches utilize different tools to address the topic in different ways, but they share significant common limitations, the two major ones being that many metabolites contained in the investigated extracts remain unidentified and the vast majority of recovered metabolites identified after important time-consuming work correspond to already known structures. Great research efforts in progress to avoid this frequent problem of ''rediscovery'' of known structures have led to the development of novel promising **dereplication methods**.

The term "**dereplication**" refers to the rapid detection and identification of known structures in crude molecular mixtures. These strategies consist of i) capturing spectral fingerprints of a sample series with a high resolution analytical system, ii) highlighting spectral similarities, patterns or discriminant signals across samples with appropriate algorithms or data mining tools [27], and iii) elucidating metabolite structures with the help of spectral libraries (**Figure 3**). These strategies are increasingly used in natural product research and provide interesting perspectives for the cosmetic industry because they don't require huge time or technical resources [28]. Currently, the analytical step of a dereplication strategy entails mainly performing liquid chromatography-mass spectrometry (LC-MS) or nuclear magnetic resonance (NMR), with each providing specific advantages with respect to sensitivity, reproducibility, resolution or sample preparation [29-32]. The strength of the procedure always relies on the integration of the obtained spectra and computational treatments in order to detect spectral patterns, correlations and/or discriminations between signals across the samp-

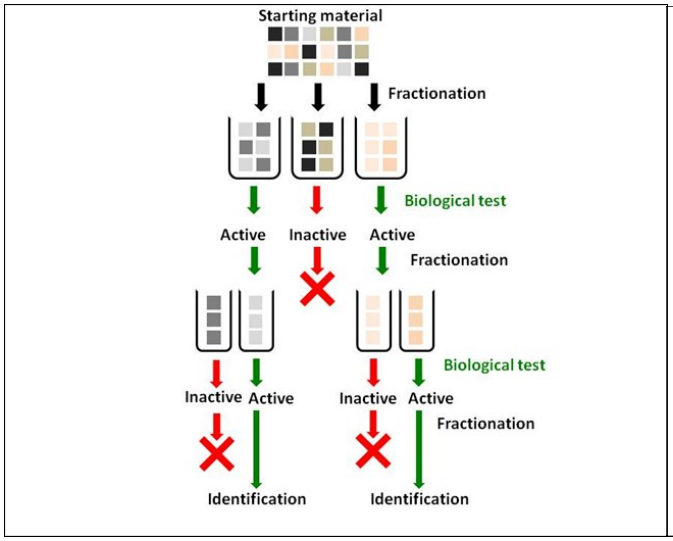

Figure 2 Schematic workflow of bioactivity-guided fractionation procedures

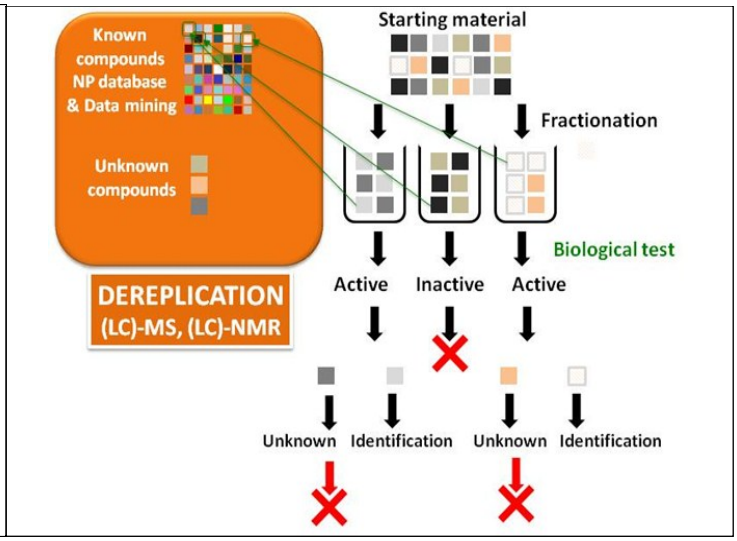

Figure 3 General workflow of natural extract dereplication approaches

les under investigation. Once relevant molecular skeletons have been highlighted, comprehensive databases containing structural features and spectral assignments are finally used to search for, match and identify the metabolite structures.

IDENTIFICATION OF METABOLITES IN NATURAL COSMETIC INGREDIENTS: A PROMISING PATTERN RECOGNITION STRATEGY BASED ON ^{13}C NMR

Here, we would like to present in more details a recently developed ^{13}C NMR-based dereplication strategy which was specifically designed for an early application in cosmetics. The methodology is illustrated by two real-life applications to plant extracts which are currently exploited as cosmetic and perfume ingredients.

General strategy

The first step of this dereplication method is to produce a series of successive fractions from a crude extract using a liquid-liquid separation system, thus exploiting the predictable wide polarity range of metabolites in the extract. In a second step, the fractions with simplified chemical composition are analyzed by ^{13}C NMR. To date, the use of ^{13}C NMR for profiling plant extracts has remained largely unexplored mainly because of its low detection sensitivity. However, ^{13}C NMR provides strong advantages for the analysis of complex mixtures because carbon atoms represent a significant part of all organic molecules. In addition, each ^{13}C position in a structure corresponds to a single signal in a ^{13}C NMR spectra and the ^{13}C NMR spectral window is large enough to obtain a good signal dispersion and reduced overlaps unlike what is frequently observed in ^{1}H NMR spectra of natural products. Moreover, high magnetic field NMR spectrometers and cryogenic probes today enable the acquisition of ^{13}C spectra with good sensitivity in a reasonable time. In a third step, all detectable ^{13}C signals in each fraction are collected and aligned across all spectra of the fraction series. The principle is to divide the ^{13}C spectral width (from 0 to 200 ppm) into regular bins ($\Delta\delta$ = 0.2 ppm) and place the absolute intensity of each ^{13}C peak in the corresponding bin. Hierarchical clustering analysis (HCA) is then performed in the resulting table in order to highlight the statistical correlations within the whole dataset. HCA is an unsupervised pattern recognition method enabling the detection of chemical shift similarities within the fraction series. As a result, statistically correlated "^{13}C signal groups" belonging to the same molecular structure are visualized in a dendrogram as clusters. Each cluster is finally assigned to a molecular structure with the help of a ^{13}C NMR data-

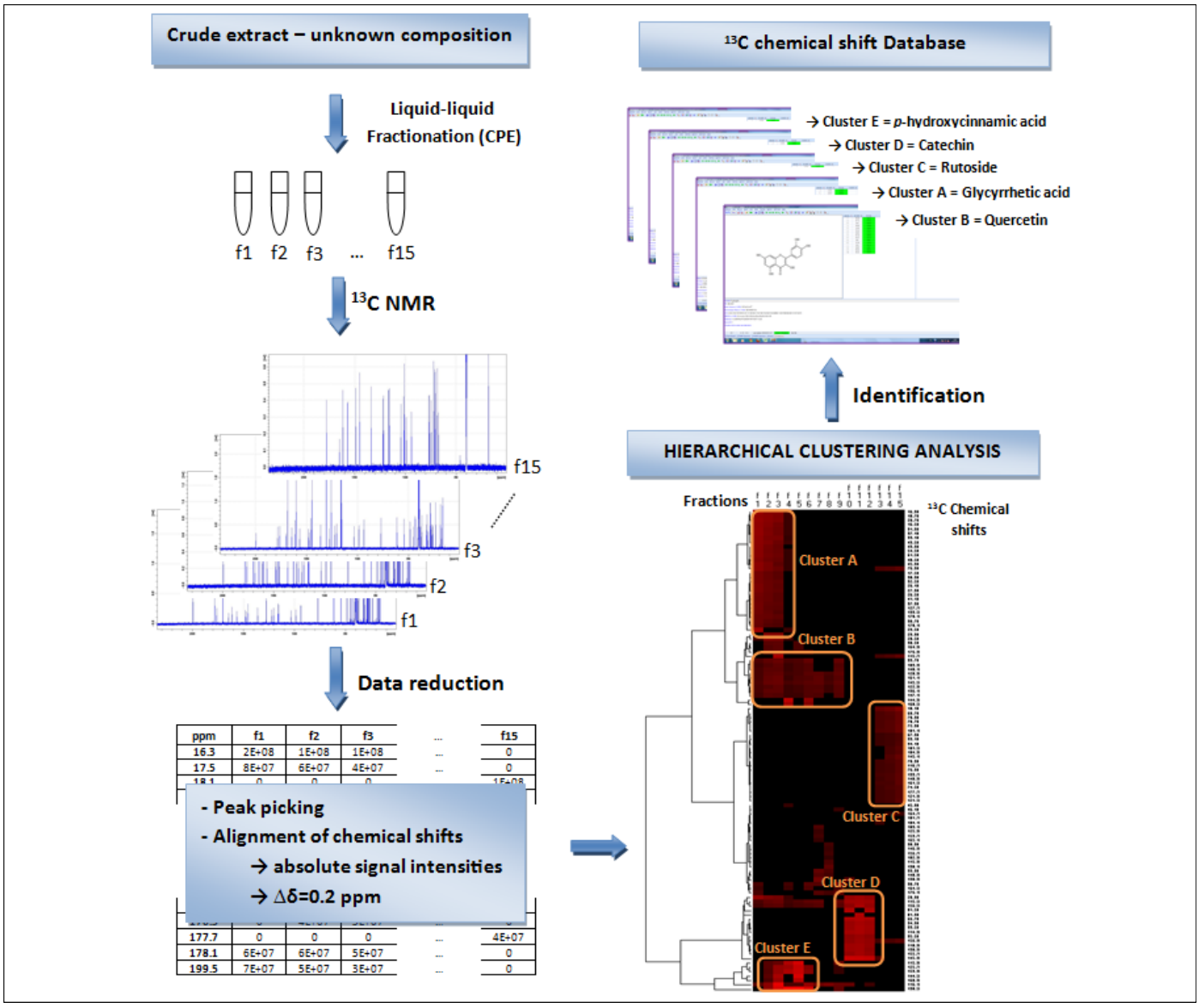

Figure 4 Natural extract dereplication strategy based on 13C-NMR pattern recognition

base that contains the structures and predicted ^{13}C NMR chemical shifts of all the compounds found in the literature for the organism (plant, marine extract, bacteria, etc.) under examination. The global workflow is illustrated in **Figure 4**, and the methodology was described in detail in a recent paper [33].

Example 1: Chemical dereplication of a crude bark extract

The strategy was firstly applied to a crude bark extract of the African tree *Anogeissus leiocarpus* Guill & Perr (Combretaceae). The bark and leaves are traditionally used as an antimalarial remedy [34]. In European countries, the ethanol-soluble fraction of the bark has found applications in the cosmetic industry as a skin protective ingredient [35]. As in most bark extracts, tannins are predominant in the ethanol-soluble part (» 80 % w/w). However, a range of other potentially interesting compounds may also be present in significant amounts. The objective here was thus to rapidly identify these minor compounds in order to assess the global composition of the extract.

In a single 95 min run, 5 g of the crude extract were first fractionated by centrifugal partition extraction (CPE), resulting in a series of 20 simplified fractions of decreasing polarity. CPE is a solid support free liquid-liquid separation technique directly derived from centrifugal partition chromatography (CPC) and which can selectively produce simplified mixtures of natural compounds from crude extracts on a multi-gram scale and in a short time [36]. The water-soluble tannins were all recovered in the last fraction which was not taken into account for the spectral data classification. The mass of each recovered fraction (at least 20 mg) was largely sufficient to achieve ^{13}C NMR spectra acquisition within 10 min. Running HCA on the aligned ^{13}C NMR data, exactly as described above, resulted in the formation of several well-defined chemical shift clusters, as visible in **Figure 5**. The HCA map was composed of 19 columns corresponding to the successive CPE fractions and 241 rows corresponding to the ^{13}C chemical shift values detected in at least one fraction. Clusters of ^{13}C chemical shifts were finally assigned to their corresponding molecular structures with the help of a locally built ^{13}C NMR chemical shift database, resulting in seven unambiguously identified compounds, namely sericoside, trachelosperogenin E, ellagic acid, an epimer mixture of (+)-gallocatechin and (-)-epigallocatechin, 3,3'-di-O-methylellagic acid 4'-O-xylopyranoside, 3,4,3'-tri-O-methylflavellagic acid 4'-O-glucopyranoside, and 3,4,3'-tri-O-methylflavellagic acid, respectively.

This first example demonstrates that despite its inherently low sensitivity ^{13}C NMR integrated with appropriate data mining tools is efficient for the characterization of natural metabolites in complex mixtures. Combining a rapid multigram-scale fractionation method with ^{13}C NMR and HCA visualization of the whole dataset resulted in direct recognition of chemical shift clusters even for substances of very similar structure.

Example 2: Chemical dereplication of depsides from the lichen *Pseudevernia furfuracea*

Pseudevernia furfuracea (L.) Zopf (Parmeliaceae) is a well-investigated foliose lichen growing on the bark of coniferous trees and widely used in the perfume industry as a fragrance or for the preservation of odors [37]. As most lichens, this species produces a diversity of secondary metabolites, among them the depsides, which are comprised of two or more hydroxybenzoic acid units linked by ester, ether or C-C-bonds. During classic solid support-based purification processes, depsides are often hydrolyzed and in many cases time-consuming procedures result only in isolation of the decomposition products and thus in misidentification of the native structures.

The objective here was to use the same above-described ^{13}C-NMR-based dereplication strategy to characterize depsides and depsidones from *P. furfuracea* directly in mixtures in an attempt to avoid extensive purification steps while maintaining metabolite structure integrity. Since depsides can be protonated or deprotenated by varying the pH, a pH-zone refining method was developed using centrifugal partition chromatography (CPC) to fractionate the initial crude sample [38, 39]. The metabolites recovered as simplified mixtures in the CPC-generated fractions (n=12) were analyzed by ^{13}C NMR and the spectral data were aligned across fractions. HCA was subsequently applied to the whole dataset, resulting again in efficient clustering of ^{13}C NMR signals, as shown in **Figure 6**. Each cluster was assigned to its corresponding molecular structure by searching the locally developed ^{13}C NMR database of depsides and depsidones. The search revealed six unambiguously identified compounds, namely methyl β-orcinolcarboxylate, atranorin, 5-chloroatranorin, olivetol carboxylic acid, olivetoric acid and olivetonide. This second example again demonstrates that the workflow based on ^{13}C NMR chemical shift pattern recognition is effective for rapid characterization of prefractionated plant extracts [38].

CONCLUSION

Currently, great interest in the use of natural active ingredients has been expressed in the cosmetic industry. Their use, however, remains strongly hampered by their complex

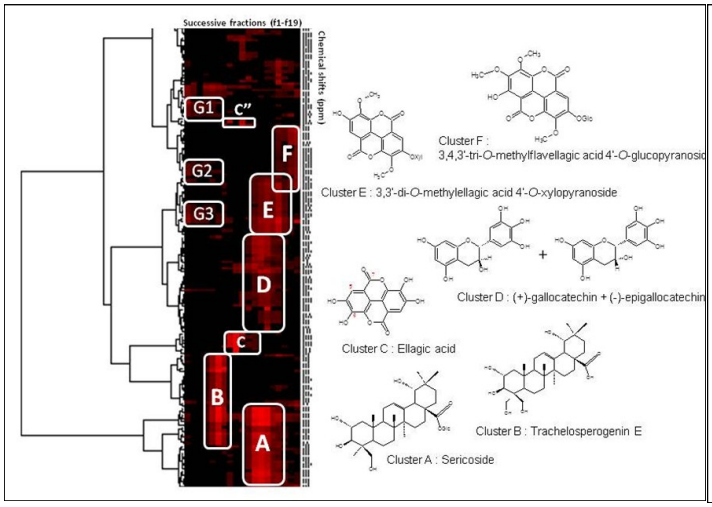

Figure 5 ^{13}C NMR chemical shift clusters obtained from the crude bark extract of Anogeissus leiocarpus

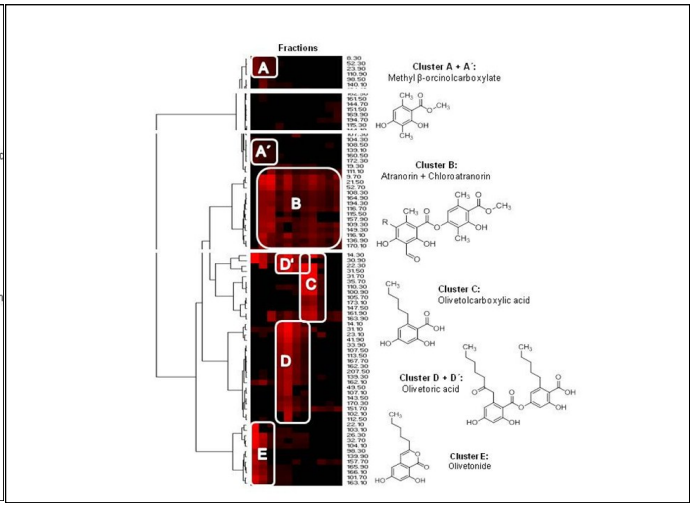

Figure 6 ^{13}C NMR chemical shift clusters obtained from a crude lichen extract (Pseudevernia furfuracea)

chemical profiles, which are difficult to characterize and standardize. We have seen in this overview that a range of analytical strategies have been developed over the last years to address these characterization issues. Among them, fingerprint analyses and bioactivity-guided fractionation procedures remain by far the most commonly used approaches. With the technological advances in off-line hyphenation of analytical systems with computational treatments and data mining tools, promising efficient methods are continually emerging. However, efforts need to be sustained to make these dereplication strategies routinely applicable in the cosmetic industry, in particular with regard to spectral libraries (MS or NMR), which today are widely fragmented and scattered as "locally built" databases in many academic and private laboratories.

ACKNOWLEDGEMENTS

The authors thank the Soliance Company, CNRS, Ministry of Higher Education and Research, and "Champagne-Ardenne DRRT" for financial support. The EU program FEDER for the PlAneT CPER project and the EU-Marie-Curie Action for the IAPP/FP7-PEOPLE "Natprotec" project are also gratefully acknowledged.

REFERENCES

[1] http://www.euromonitor.com/beauty-and-personal-care.

[2] Du, B., Bian, Z., and Xu, B., Skin health promotion effects of natural beta-glucan derived from cereals and microorganisms:a review, Phytother Res, 28 (2014) 159-66.

[3] Morganti, P., and Morganti, G., Chitin nanofibrils for advanced cosmeceuticals, Clin Dermatol., 26 (2008) 334-340.

[4] Kim, K.C., Kim, Y.H., Kim, K.S., Han, C.S., and Kim, C.H., Cosmeceutical properties of levan produced by Zymomonas mobilis., J Cosmet Sci, 56 (2005) 395-406.

[5] Martini, M.C., and Seiller, M.. Actifs et additifs en cosmétologie, Lavoisier, Paris, France, 2006, 3rd Edition

[6] Nichols, J.A., and Katiyar, S.K., Skin photoprotection by natural polyphenols: anti-inflammatory, antioxidant and DNA repair mechanisms, Arch Dermatol Res., 302 (2010) 71-83.

[7] Epstein, H., Cosmeceuticals and polyphenols, Clin Dermatol., 27 (2009) 475-478.

[8] Van Breeman, R.B., Fong, H.H., and Farnsworth, N.R., The role of quality assurance and standardization in the safety of botanical dietary supplements, Chem Res Toxicol., 20 (2007) 577-582.

[9] Gao, X.H., Zhang, L., Wie. H., and Chen, H.D., Efficacy and safety of innovative cosmeceuticals, Clin Dermatol., 26 (2008) 367-374.

[10] http://ec.europa.eu/enterprise/sectors/chemicals/reach/index_en.htm.

[11] Salgueiro, L., Martins, A.P., and Correia, H.. Raw materials: the importance of quality and safety. A review, Flavour and Fragrance Journal, 25 (2010) 253-271.

[12] McLaughin, J.L., and Rogers, L., The use of biological assays to evaluate botanicals, Drug Inf J., 32 (1998) 513-534.

[13] Nuzzo, G., Gallo, C., Ippolito, G., Cutignan,o A., Sardo, A., and Fontana, A., Composition and Quantitation of Microalgal Lipids by ERETIC 1H NMR Method, Mar Drugs, 11 (2013) 3742-3753.

[14] Pan, T., and Wang, P.W., Aljuffali, I.A., Leu, Y.L., Hung, Y.Y., Fang, J.Y., Coumarin derivatives, but not coumarin itself, cause skin irritation via topical delivery, Toxicol Lett., 226 (2014) 173-81.

[15] Shewiyo, D.H., Kaale, E., Risha, P.G., Dejaegher, B., Smeyers-Verbeke, J., and Vander Heyden Y., HPTLC methods to assay active ingredients in pharmaceutical formulations: a review of the method development and validation steps, J Pharm Biomed Anal., 66 (2012) 11-23.

[16] Sun, S., Chen, J., Zhou, Q., Lu, G., and Chan, K., Application of mid-infrared spectroscopy in the quality control of traditional Chinese medicines, Planta Med., 76 (2010) 1987-1996.

[17] Sarker, S.D., and Nahar, L., Hyphenated techniques and their applications in natural products analysis, Methods Mol Biol., 864 (2012) 301-340.

[18] Fiehn, O., Metabolomics - the link between genotypes and phenotypes, Plant Mol Biol., 48 (2002) 155-171.

[19] Zhang, A.H., Sun, H., Wang, P., Han, Y., and Wang, X.J., Modern analytical techniques in metabolomics analysis, Analyst, 137 (2012) 293-300.

[20] Sheridan, H., Krenn, L., Jiang, R.W., Sutherland, I., Ignatova, S., Marmann, A., Liang, X.M., and Sendker, J., The potential of metabolic fingerprinting as a tool for the modernisation of TCM preparations, J Ethnopharmacol., 140 (2012) 482-491.

[21] Agarwal, A., D'Souza, P., Johnson, T.S., Dethe, S.M., and Chandrasekaran, C., Use of in vitro bioassays for assessing botanicals, Curr Opin Biotechnol., 25 (2014) 39-44.

[22] Cos, P., Vlietinck, A.J., Berghe, D.V., and Maes, L., Anti-infective potential ofnatural products: how to develop a stronger in vitro 'proof-of-concept', J Ethnopharmacol., 106 (2006) 290-302.

[23] Cheng, Z., Wu, T., TLC bioautography: high throughput technique for screening of bioactive natural products, Comb Chem High Throughput Screen, 16 (2013) 531-549.

[24] Ma, X.H., Zheng, C.J., Han, L.Y., Xie, B., Jia, J., Cao, Z.W., Li, Y.X., and Chen, Y.Z., Synergistic therapeutic actions of herbal ingredients and their mechanisms from molecular interaction and network perspectives, Drug Disc Today, 14 (2009) 579-588.

[25] Wagner, H., Synergy research: Approaching a new generation of phytopharmaceuticals, Fitoterapia, 82 (2011) 34-37.

[26] Houghton, P.J., Howes, M.J., Lee, C.C., and Steventon, G., Uses and abuses of in vitro tests in ethnopharmacology: visualizing an elephant, J Ethnopharmacol., 110 (2007) 391-400.

[27] http://en.wikipedia.org/wiki/List_of_open-source_bioinformatics_software.

[28] Kersten, R.D., and Dorrestein, P.C., Secondary Metabolomics: Natural Products Mass Spectrometry Goes Global, Acs Chem Biol., 4 (2009) 599-601.

[29] Forner, D., Berrue, F., Correa, H., Duncan, K., and Kerr, R.G., Chemical dereplication of marine actinomycetes by liquid chromatography-high resolution mass spectrometry profiling and statistical analysis, Anal Chim Acta, 805 (2013) 70-79.

[30] Klitgaard, A., Iversen, A., Andersen, M.R., Larsen, T.O., Frisvad, J.C., and Nielsen, K.F., Aggressive dereplication using UHPLC-DAD-QTOF: screening extracts for up to 3000 fungal secondary metabolites, Anal Bioanal Chem., 406 (2014) 1933-43.

[31] Halabalaki, M., Vougogiannopoulou, K., Mikros, E., and Skaltsounis, A.L., Recent advances and new strategies in the NMR-based identification of natural products, Curr Opin Biotechnol., 25 (2014) 1-7.

[32] Qiu, F., McAlpine, J.B., Lankin, D.D., Burton, I., Karakach, T., Chen, S.N., and Pauli, G.F., 2D NMR Barcoding and Differential Analysis of Complex Mixtures for Chemical Identification: The Actaea Triterpenes, Anal Chem., 86 (2014) 3964-72.

[33] Hubert, J., Nuzillard, J.M., Purson, S., Hamzaoui, M., Borie, N., Reynaud, R., and Renault, J.H., Identification of Natural Metabolites in Mixture: A Pattern Recognition Strategy Based on C-13 NMR, Anal Chem., 86 (2014) 2955-2962.

[34] Vonthron-Senecheau, C., Weniger, B., Ouattara, M., Bi, F.T., Kamenan, A., Lobstein, A., Brun, R., and Anton, R., In vitro antiplasmodial activity and cytotoxicity of ethnobotanically selected Ivorian plants, J Ethnopharmacol., 87 (2003) 221-225.

[35] Corstjens, H., Clio, D., Neven, A., Declercq, L., and Yarosh, D.B., Anogeissus leiocarpus extract acts as a (photo)ageing repair ingredient in an ex vivo human skin model, J Inv Dermatol., 131 (2011) S32-S32.

[36] Hamzaoui, M., Renault, J.H., Nuzillard, J.M., Reynaud, R., and Hubert, J., Stepwise elution of a three-phase solvent system in centrifugal partition extraction: A new strategy for the fractionation and phytochemical screening of a crude bark extract 2013, Phytochem Anal., 24 367-73.

[37] Joulain, D., and Tabacchi, R., Lichen extracts as raw materials in perfumery, Part 2: treemoss, Flav Fragr J., 24 (2009) 105-116.

[38] Oettl, S.K., Hubert, J., Nuzillard, J.M., Stuppner, J., Renault, J.H., and Rollinger, J.M., Dereplication of depsides from the lichen Pseudevernia furfuracea by centrifugal partition chromatography combined to 13C nuclear magnetic resonance pattern recognition, Anal Chim Acta, 2014 in press.

[39] Hamzaoui, M., Renault., J.H., Reynaud, R., and Hubert, J., Centrifugal Partition Extraction in the pH-zone refining displacement mode: An efficient strategy for the screening and isolation of bioactive phenolic compounds, J Chromatogr B., 937 (2013) 7-12

Corresponding author
email: jane.hubert@univ-reims.fr

The Skin Firming "Red-volution": Anti-cellulite Efficacy of a *Papaver rhoeas* Extract

THIERRY BALDECCHI[1], LILIA HEIDER[2], MARINA LEFORT[2], CHRISTOPHE CAROLA[2], CLAUDIA CARTIGLIANI[3], ADRIANA BONFIGLI[3] and FRANK PFLUECKER[2]

[1)] Merck Chimie SAS, 201 rue Carnot, 94126 Fontenay-sous-Bois, France, Contact : +33.143945485 or [2)] Merck KGaA, Frankfurter Strasse 250, 64293 Darmstadt, Germany [3)] ISPE srl - Institute of Skin and Product Evaluation, Via Bruschetti 1, 20125 Milano, Italy

This publication was presented as a poster presentation at the 28th IFSCC Congress, October 27-30, 2014, Paris, France

Keywords: Anti-cellulite, Papaver rhoeas extract, poppy seed, skin firming, adipocyte, blood microcirculation

ABSTRACT

The intention of this paper is to report the in vivo efficacy of a natural active ingredient based on the seeds of a special poppy species. This Papaver rhoeas extract can significantly increase skin blood micro-flow and flatten the dermo-hypodermal junction, leading to a visual improvement of cellulite conditions. The study confirms the outcome of several in vitro and ex vivo investigations in which the extract displayed both prevention of lipogenesis and activation of lipolysis. This set of results demonstrates that this natural ingredient may offer an attractive option for the design of skin firming, skin shaping, face contouring or anti-cellulite cosmetic products.

INTRODUCTION

Cellulite is an important concern affecting a majority of women dreaming of a perfect skin appearance and body shape. This phenomenon refers to a local alteration of the skin which acquires a characteristic unappealing and uneven skin aspect usually described as an orange peel or a mattress appearance. Cellulite is a complex pathology which affects at least 85% of post-pubertal women [1, 2] and is commonly seen in thighs, hips, and buttocks but can also affect other areas including the abdomen. The underlying causes of cellulite can be found in the number, size and conformational arrangement of the adipocytes (fat cells) localized beneath the dermis and within the surrounding collagen matrix and aqueous environment [3]. Cellulite occurs when too many adipose cells reach an excessive size due to their large lipid content, or are hypertrophied. When this phenomenon reaches a certain stage, the hypertrophy induces compression of the blood vessels resulting in reduced blood flow and water infiltration in the hypodermis [4]. Hormones are also known to play a significant role in the appearance of cellulite [5]: estrogen stimulates lipogenesis (synthesis of triglycerides within adipocytes) and inhibits lipolysis (breakdown of lipids and hydrolysis of triglycerides into free fatty acids and glycerol release), which finally results in an increase of adipocyte size.

A new, natural ingredient shows interesting activities at the adipocyte level. It is extracted from the seeds of *Papaver rhoeas*, better known as corn poppy, corn rose, field poppy, red poppy or coquelicot. Abundant in nature, this plant has between 50 and 120 different known species worldwide. The flower is large and showy, with four vivid red petals, most commonly seen with a black spot at their base. The red wild form is often grown as an ornamental plant but this is not its only application: petal extracts are said to be able to soothe coughs and seeds can be used as a food ingredient or for oil production [1, 6].

The search for new, natural and sustainable cosmetic active ingredients encouraged us to evaluate the potential of *Papaver rhoeas* extract for cosmetic use. Existing *in vitro* and *ex vivo* studies have demonstrated that *Papaver rhoeas* extract is able to inhibit the activity of the specific enzyme glycero-3-phosphate dehydrogenase (G_3PDH) and boost the release of free fatty acids, leading to a proven decrease in size of adipocytes [7].

EXPERIMENTAL

Materials and methods

Flowers of *Papaver rhoeas* are cultivated in Europe and North America. The seeds, provided by Greenpharma S.A.S., Orleans, France, are processed via a supercritical CO_2 extraction with ethanol as cosolvent. This process is classified as a sustainable approach because it is physiologically harmless and environmentally friendly CO_2 can be recycled within the production plant. After evaporation of the cosolvent, a standardized extract of *Papaver rhoeas* is obtained under given process conditions. The lead component of the extract is linoleic acid in a concentration range between 69 – 85%. Other components include oleic acid, palmitic acid and other saturated fatty acids bound or in free form. Although the poppy species *Papaver rhoeas* is not known to contain any alkaloids, the seed extract was nonetheless analyzed and found to be free of alkaloids. To obtain a ready-to-use, easy-to-formulate cosmetic active ingredient, the poppy seed extract is then mixed with a suitable cosmetic oil (INCI: Caprylic/Capric Triglyceride). The final ingredient is a clear oil containing 10% *Papaver rhoeas* extract.

To enrich the set of *in vitro* and *ex vivo* data, a randomized double-blind clinical study was conducted for 56 days to investigate the efficacy of *Papaver rhoeas* extract in treating cellulite inesthetisms [8]. An oil-in-water emulsion containing 0.1% *Papaver rhoeas* extract was compared with a placebo cream (identical to the *verum* except for the poppy extract) (***Figure 1***). Both creams contained no other known anti-cellulite actives such as caffeine. The test was carried out according to the Declaration of Helsinki on 22 Caucasian female volunteers, average age 46.0 years. Volunteers were informed of the nature, purpose and risk of the study and gave their written consent before participating in the test. The selection of volunteers was carried out according to previously agreed inclusion criteria including age (18 to 60 years), Body Mass Index (less than 30), presence of cellulite on their thighs and/or gluteus (degree 1 to 3 according to Nurnberger and Muller scale with evaluation done by pinch test [9, 10]) and commitment not to use additional anti-cellulite treatments - either topical and/or systemic - for the duration of the study.

Products to be tested were applied to the volunteers' thighs and gluteus. The participants were asked not to wash their thighs for 2 hours before the measurements and not to apply any products for 12 hours before the baseline visit. Participants applied the active emulsion twice a day for 8 weeks to one thigh and the placebo emulsion to the other thigh. The side of application of the two

emulsions (left or right) was randomized among the volunteers: each sample was labeled "right" or "left", indicating the side of application of the product. The assignment of subject number and subsequent placement on the randomization chart were made in the order of appearance at the study center on the first day. The products were given to the subjects in anonymous containers that provided no information about the treatment.

The extent of anti-cellulite efficacy was assessed by the skin firmness and skin elasticity (Cutometer® MPA 580 by Courage + Khazaka Electronic GmbH, Cologne, Germany), skin replicas and image analysis (Quantilines software from Monaderm (SAM), Monaco), skin blood micro-flow measurement (laser Doppler device Periflux PF4001 from Perimed AB, Järfälla, Sweden) and measurement of the length of the dermo-hypodermal junction (high frequency ultrasound scanner Dermascan® C Ver.3 from Cortex Technology, Hadsund, Denmark). Furthermore, digital images of the volunteers were taken at each control time (Fotofinder Dermoscope® Ver. 2.0 from Fotofinder Systems GmbH, Bad Birnbach, Germany). At the beginning of the test and after 4 and 8 weeks of treatment, instrumental evaluations were carried out on the thighs, below the fold of the gluteus. All measurements were done in a temperature and humidity controlled room (24 ± 2 °C; 50 ± 10 % R.H.).

Skin elasticity

The cutometer is a device which measures the vertical deformation of the skin when sucked into the opening of a measuring probe by a constant level of depression (350 mbar) for an established time (1 second). The air depression is then annulled and the released skin can return to its original position. Three suction/release cycles are performed on the same point and are plotted in axes where the deformation of the skin (expressed in mm) is a function of time (expressed in seconds). Deformation parameters relating to the elastic features of the skin can then be measured. The following parameters have to be considered:

- Parameter R0 is the maximal deformation of the skin (noted U_f). The smaller the value, the better.
- Parameter R2 is the overall elasticity. It is equal to the ratio U_a / U_f where U_a is the total deformation recovery at the end of the stress-off period. The closer the value is to 1, the more elastic the skin.
- Parameter R6 is the viscoelastic ratio U_v / U_e, where U_v is the viscoelastic creep occurring after the elastic deformation and U_e is the elastic deformation obtained during the stress period. The smaller this value, the higher the skin elasticity.

Skin smoothness

Negative imprints of the skin surface (skin replicas) are obtained by allowing a fast hardening synthetic polymer to dry on adhesive discs. The skin replicas are then analysed by an image-processing software which allows a global data analysis of some relief parameters. Each silicone replica of the cutaneous surface is illuminated by a light source with a defined incident angle (35°) in order to generate shadows: the higher the furrows, the wider the shadows. An image covering a 12 x 9 mm area of each skin replica surface is acquired with a high performance CCD video camera. The software allows measurement of the following parameters:

- Parameter Ra: average roughness of the profile
- Parameter Rz: average maximum roughness (average difference between the highest and lowest point in five sections of the profile).

Ra and Rz are reported in units of brightness (grey levels) ranging from 0 to 255. The efficacy of the product in improving skin smoothness is evidenced by a decrease in Ra and/or Rz values at the end of the treatment.

Skin blood micro-flow

The blood micro-flow is measured by means of a computerized laser Doppler device. A laser light, carried by an optic fiber probe, is partially reflected and partially absorbed by the examined tissue. The light hitting the moving hematic cells is subject to wavelength variation (Doppler effect), while the light hitting static bodies does not change its wavelength. The power and frequency distribution of the wavelength variations is correlated to the number and the speed of the hematic cells, but not to their direction. The relative information is picked up by a return optic fiber, converted into an electronic signal, and analyzed. The perfusion is expressed in Perfusion Units (P.U.), which are arbitrary units of the laser Doppler device. The higher the value, the greater the blood flow is.

Length of the dermo-hypodermal junction

The use of a high-resolution scanner emitting high-frequency ultrasound (20MHz) allows observation of the tissue down to a depth of 15 mm with 60 µm axial and 200 µm lateral resolution. The device is based on the physical principle of ultrasound emission by a transducer. When an ultrasound beam reaches the skin, it goes through structurally different sections, since the beam is partly transmitted and partly reflected by the limiting areas of the adjacent skin sections. Echo sounds of different amplitude are thus generated. Their intensity is then assessed by a microprocessor and shown on the screen. The intensity of the reflection is expressed by means of a scale of grey shades or pseudo colors, where the color changes according to the intensity of the reflected signal: white > yellow > red > green > blue > black. For example, a heterogeneous body generates numerous echo sounds and is therefore displayed in white, while a homogeneous one does not generate echo sounds and is displayed in a dark shade. Analysis of the images provides some information on the structural and morphologic characteristics of the different skin structures (epidermis, dermis and hypodermis). The parameter length of the dermo-hypodermal junction (in millimeters) is measured for each ultrasound images. In case of

		Placebo	Verum (contains 0,1% *Papaver rhoeas* extract)
Phase A	**RonaCare® Poppy SE: CAPRYLIC/CAPRIC TRIGLYCERIDE, PAPAVER RHOEAS EXTRACT, TOCOPHEROL**	**0,00**	**1,00**
	ARACHIDYL ALCOHOL, BEHENYL ALCOHOL, ARACHIDYLGLUCOSIDE	3,00	3,00
	ISONONYL ISONONANOATE	2,00	2,00
	CAPRYLIC/CAPRIC TRIGLYCERIDE	**2,00**	**1,00**
	DICAPRYLYL CARBONATE	3,00	3,00
	BUTYLENE GLYCOL COCOATE	2,00	2,00
Phase B	AQUA (WATER)	79,20	79,20
	PROPYLENE GLYCOL	6,00	6,00
Phase C	HYDROXYETHYL ACRYLATE/SODIUM ACRYLOYLDIMETHYLTAURATE COPOLYMER, SQUALANE, POLYSORBATE 60	2,00	2,00
Phase D	PRESERVATIVE	0,80	0,80
	pH (25°C)	5,4	5,3
	Viscosity in mPa.s (25°C, Brookfield LV, Sp.C, 10rpm)	22000	20000

Figure 1: Composition of the placebo and the test formulation with Papaver rhoeas extract (verum).

cellulite, the excess subcutaneous fat bulges into the dermis (protrusion of adipose tissue toward the dermis). This phenomenon is called "herniation of the dermo-hypodermal junction". The efficacy of the treatment is shown by a linearization of the dermo-hypodermal junction and thus a decrease of its length.

Statistical analysis

Mean values, standard deviations, variations and percentage variations were calculated for each set of values. The instrumental data (T0, T4weeks and T8weeks) were statistically compared by means of repeated measures ANOVA and Bonferroni Test for dependent and parametric data, while the variations were statistically compared by means of t-test for parametric and dependent data groups. The groups of data were considered statistically different for a probability value $p < 0.05$.

RESULTS AND DISCUSSION

Because one person dropped out of the study for reasons unrelated to the products used, the results refer to 21 volunteers. The *in vivo* results are based on an 8-week period with control times at the beginning and after 4 and 8 weeks of treatment.

Skin elasticity

At both control times application of an emulsion containing 0.1% of *Papaver rhoeas* extract to human volunteers induced statistically significant improvements ($p<0.05$) in all three viscoelasticity parameters (decrease of maximal deformation R0 and viscoelastic ratio R6, increase of overall elasticity R2), whereas the placebo could only improve parameter R2 representing the overall elasticity. These results highlight an improvement in the biomechanical elasticity of the skin when treated with the test product. The skin can recover its structure better after deformation and can be considered firmer than before.

Skin smoothness

Statistically significant improvements ($p<0.01$) in all skin smoothness parameters (average roughness Ra and average maximum roughness Rz) were detected after 4 and 8 weeks of application of both the placebo cream and the test cream. Although the skin treated with the cream containing *Papaver rhoeas* extract was smoother than before treatment, this was true also of the skin treated with placebo. This could be attributable to the fact that the base formulation already has a high moisturizing and smoothing potential.

Skin blood micro-flow

Unlike the placebo cream, which after application had no statistical influence on this parameter, the emulsion containing 0.1% of *Papaver rhoeas* extract induced a statistically significant increase ($p<0.01$) after 4 and 8 weeks (increase by approx. 10% and 16% respectively) relative to the baseline. Moreover, comparison of the active product and the placebo showed a statistically significant difference after 8 weeks of treatment ($p<0.05$) (***Figure 2***). Stimulation of microcirculation is considered a key parameter in cellulite treatment. It is believed to be the first step in fighting cellulite, as it activates the removal of accumulated fluids and toxic elements. Moreover, it can improve the interstitial matrix basal regulation and fibroblast activity, and decrease interstitial edema, with a subsequent increase in lipolysis and a better oxygen supply and nutrition of the adipose tissue [11].

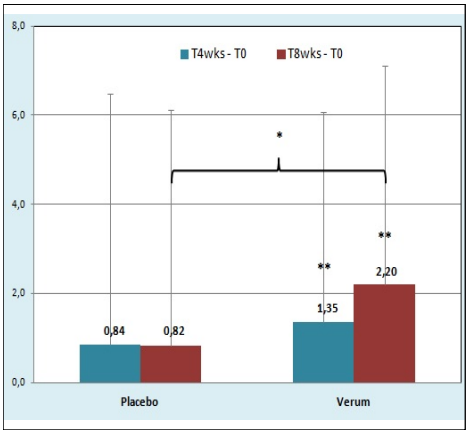

Figure 2: Evolution of skin blood micro-flow (P.U.) after 4 and 8 weeks of treatment with an emulsion containing 0.1% Papaver rhoeas extract or with a placebo cream (*=p<0.05; **=p<0.01)

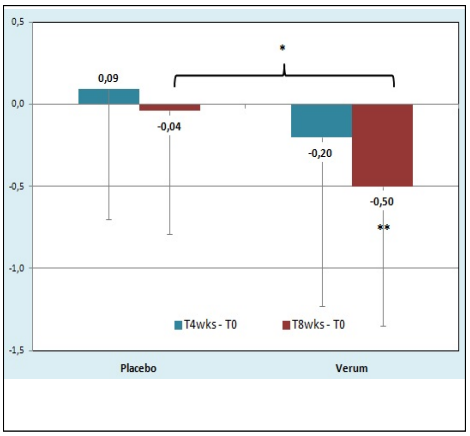

Figure 3: Evolution of the length of the dermo-hypodermal junction (mm) after 4 and 8 weeks of treatment with an emulsion containing 0.1% Papaver rhoeas extract or with a placebo cream (*=p<0.05; **=p<0.01)

Length of the dermo-hypodermal junction

The study showed a linearization of the dermo-hypodermal interface, with a statistically significant decrease in its length after 8 weeks ($p<0.01$) in the area treated with the cream with 0.1% of *Papaver rhoeas* extract. Application of the placebo emulsion did not induce any significant variation in the measured parameter. Furthermore, the statistical comparison between the active product and the placebo evidenced a statistically significant difference after 8 weeks of treatment ($p<0.05$) (***Figure 3***).

The efficacy of the treatment with an emulsion containing 0.1% of *Papaver rhoeas* could in addition be depicted using ultrasound images. After 4 and 8 weeks, the dermo-hypodermal junction became visibly flatter (***Figure 4***). This was linked with a decrease in the number and/or size of excess subcutaneous adipocytes that were bulging into the dermis and thus extending the length of the junction.

Digital imaging

Instrumental measurements showed the positive impact of the poppy seed extract in fighting cellulite inesthetisms by an improvement in a wide range of parameters. These measurements could be confirmed by additional digital imaging which provided immediate insights into the evolution of the volunteers' skin aspect. A closer look at the area treated with 0.1% *Papaver rhoeas* extract showed the skin surface of the gluteus and

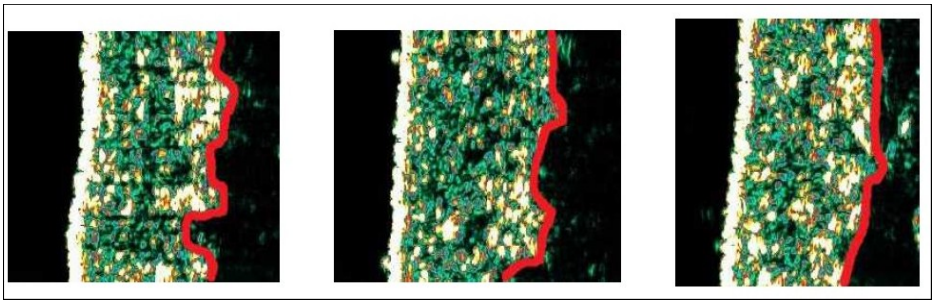

Figure 4: Ultrasound images taken before and after 4 and 8 weeks of treatment with an emulsion containing 0.1% Papaver rhoeas extract (Volunteer No. 17)

thighs to be smoother and the "orange peel" visibly reduced. In addition, the furrows seemed reduced in depth (***Figure 5***).

Figure 5: Digital images taken before and after 4 and 8 weeks of treatment with an emulsion containing 0.1% Papaver rhoeas extract (Volunteer No. 8).

CONCLUSION

Papaver rhoeas, commonly known as red poppy, is an abundant flower which has much more to offer than its beautiful and intensive red color. An innovative, natural and highly effective active ingredient could be extracted from its seeds, finally offering a solution to demanding women who want a firmer and more beautiful body shape. Clinical evaluations were carried out to prove that it indeed is an attractive option for the development of innovative skin firming, skin shaping or anti-cellulite cosmetic products.

Application of an emulsion containing 0.1% of *Papaver rhoeas* extract to human volunteers induced statistically significant improvements in all viscoelasticity parameters, all skin smoothness parameters, blood microcirculation and linearization of the dermo-hypodermal junction. Moreover, comparison of the test product and the placebo evidenced a statistically significant difference after 8 weeks of treatment for the two parameters linked most specifically with cellulite: blood micro-flow and length of the dermo-hypodermal junction. These interesting results are also visible in digital images of the treated areas where there is a clear tendency to correct cellulite inesthetisms. The results of this *in vivo* study confirm the outcome of several promising *in vitro* and *ex vivo* investigations which showed the ability of this new natural ingredient gained from the seeds of the red poppy flower to both prevent lipogenesis and activate lipolysis.

Combinations with existing cellulite improving actives like caffeine or other established ingredients could also be of interest. Based on the presented results, we suggest investigating possible synergies of such combinations to reach a higher degree of knowledge of the slimming processes and furthermore to obtain an enhanced efficacy in firming and lipolytic activity.

REFERENCES

[1] Wirth, A., Adipositas – Ätiologie, Folgekrankheiten, Diagnose, Therapie, Springer Verlag, Berlin Heidelberg, 2008, 3rd Edition

[2] Rawlings, A.W., Cellulite and its treatment, Int. J. Cosmet. Sci, 28 (2006) 175–190

[3] Lintner, K., Cellulite: Evolving technologies to fight the "orange peel" battle, Cosmetics & Toiletries, 124 (9) (2009) 74-80

[4] Avram, M.M., J. Cosmet. Laser Ther., 6 (4) (2004) 181-186

[5] Ahima, R.S., and Flier, J.S. , Trends Endocrinol. Metab., 11*(8) (2000) 327– 332*

[6] Papaver rhoeas: *http:// en.wikipedia.org/wiki/Papaver_ rhoeas (last checked on Jun. 23rd 2014)*

[7] Heider, L., Lefort, M., Carola, C., Hanau, H., Pflücker, F., Bernard, P., and Himbert, F., New cosmetic aspects of Papaver rhoeas, Household and Personal Care Today, 9 *(2) (2014) 59-63*

[8] ISPE report R212-13-01-02, Instrumental evaluation of the efficacy of a slimming product in treating cellulite inesthetisms: Double-blind study versus placebo (2013).

[9] Nürnberger, F., and Müller, G., So-called cellulite: an invented disease, J. Dermatol. Surg. Oncol., 4 (1978) 221–229

[10] Hexsel, D.M., Dal'forno, T., and Hexsel, C.L., A validated photonumeric cellulite severity scale, J. Eur. Acad. Dermatol. Venerol., Journal compilation (2009)

[11] Distante, F., Bacci, P.A., and Carrera, M., Efficacy of a multifunctional plant complex in the treatment of so-called "cellulite": Clinical and instrumental evaluation, Int. J. Cosmet. Sci. 28 (2006) 191–206

Corresponding author
email: thierry.baldecchi@merckgroup.com

Sunscreens – UV or Light Protection

J. Lademann[1], M.E. Darvin[1], H.-J. Weigmann[1], S. Schanzer[1], L. Zastrow[1], O. Doucet[2], H. Meffert[3], J. Krutmann[4], D. Kockott[5], T. Vergou[6], M.C. Meinke[1]

[1] Charité - Universitätsmedizin Berlin, Department of Dermatology and Allergology, Center of Experimental and Cutaneous Physiology (CCP), Berlin, Germany

[2] COTY LANCASTER, International R & D Center, Monaco /98000 MC

[3] Dermatologisches Zentrum Berlin, Potsdamer Chaussee 80, 14129 Berlin, Germany; hans.meffert@web.de

[4] IUF – Leibniz Research Institute for Environmental Medicine, Düsseldorf, Germany

[5] UV-Technik Hanau, Germany

[6] Hospital "A. Syggros", University of Athens, 5 Dragoumi Str., Athens 16121, Greece

Educational Review

Part of this publication was presented as a podium presentation at the 28th IFSCC Congress, October 27-30, 2013, Paris, France.

ABSTRACT

Sunscreens should provide protection against sunburn, immunosuppression and even skin cancer. Recently it could be shown that half of all free radicals induced in the skin by solar radiation have their origin in the visible and infrared spectral ranges. The high sun protection factors of modern sunscreens tempt people to expose themselves considerably longer to sunlight than if they leave their skin unprotected. Due to this prolonged exposure, radical formation in the visible and infrared spectral ranges may distinctly exceed a critical threshold. This, in turn, may lead to tissue damage at a cellular level. The present article shows methods which can be employed to protect one's body with sunscreens also in the visible and infrared spectral ranges of the sun. Moreover, standardization issues for sunscreens in the visible and infrared ranges are addressed.

INTRODUCTION

This article is based on an initiative of the Society of Dermopharmacy as a result of a session and round table discussion at the annual conference of the society in 2013.

While solar radiation is vital for life on earth, it is also one of the most dangerous environmental factors in terms of our cutaneous physiology and vital functions [1]. Sunlight decisively influences both our well-being and the indispensable vitamin D synthesis, whereas excessive doses of solar radiation induce sunburns, skin aging, immunosuppression and even skin cancer [2, 3]. The global incidence of non-melanoma skin cancer and malignant melanoma keeps increasing [4, 5]. Unless this trend can be slowed down, skin cancer will remain the most frequent type of human cancer, despite the fact that sunscreens and their protective efficacy are constantly improved.

This article addresses the issue of whether future sunscreens have to provide ultraviolet (UV) or light protection from the UV to the infrared spectral range to optimally safeguard the skin against sun exposure.

A brief outline of the history of sunscreens follows. The first commercial sunscreen was launched on the market in the first half of the last century [6]. In 1922, Eder and Freund introduced 2-naphthol-6,8-disulfonic acid salts, which were quite effective in both the UVB and UVA region. In 1956, the sun protection factor (SPF) was defined, but at that time it covered mainly the UVB spectral range. In 2006, the European Union established criteria stipulating that sunscreens must absorb both UVA and UVB radiation at a ratio of at least 1:3 [7]. If this requirement is met, the products can be labeled and sold as sunscreens. Ultraviolet filters and reflective substances like titanium dioxide are the decisive components in sunscreens, reducing the intensity of the sun's radiation reaching the viable cells of the human body. In 2012, the European Union and the European Free Trade Association harmonized the sunscreen protection classes, stipulating that a sunscreen with an SPF between 6 and 10 be labeled "low protection". Products labeled with an SPF between 15 and 25 are to be categorized "medium protection", whereas sunscreens with an SPF between 30 and 50 are to be labeled "high protection" and those with an SPF greater than 50 (SPF50+) "very high protection". This decision was based on the fact that SPF values above 50 are difficult to determine [8]. Moreover, a competition for extremely high sun protection factors up to 100 was to be avoided.

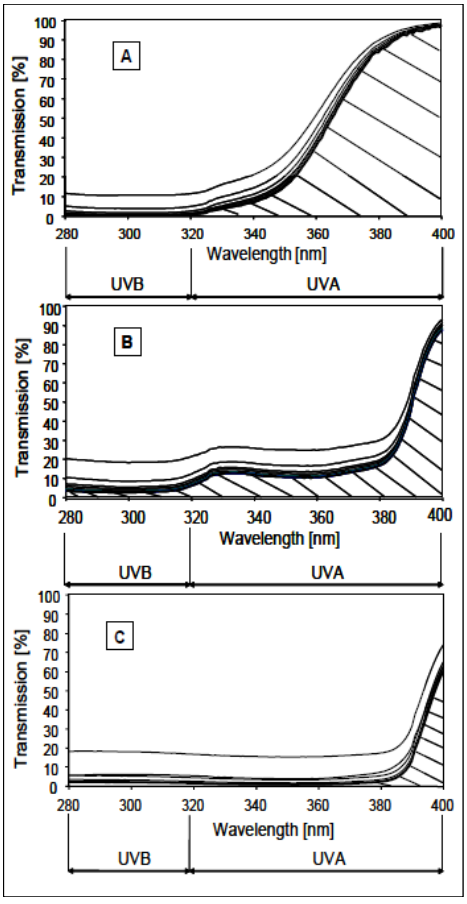

Figure 1: Spectral transmittance of sunscreens produced 10 years ago and of current sunscreens (a): spectral transmittance of a commercial sunscreen popular 10 years ago, (b): spectral transmittance of a modern sunscreen that shows very good absorption properties in both the UVB and the UVA ranges, (c): current premium products that have an excellent protective effect both in the UVB and the UVA [11].

SPECTRAL TRANSMITTANCE OF SUNSCREENS

The spectral transmittance of a sunscreen can be measured on tape strips taken after application of the sunscreen to the inner forearm [9, 10]. ***Figure 1*** provides an overview of the historical development of the spectral transmittance in sunscreens [11]. ***Figure 1a*** shows the spectral transmittance of a commercial sunscreen that was popular 10 years ago. Whereas a good protective effect is visible in the UVB range, this sunscreen provided only little protection in the UVA range. ***Figure 1b*** shows a modern sunscreen that exhibits very good absorption properties not only in the UVB but also in the UVA spectral domain. Today, there are various premium products, such as those depicted in ***Figure 1c***, which have an excellent protective effect both in the UVB and in the UVA spectrum.

OPTIMAL AMOUNT OF SUNSCREEN TO BE APPLIED TO THE SKIN

The sun protection factor (SPF) indicates how much longer people can expose their skin to the direct sunlight subsequent to sunscreen application than when their skin is left unprotected. To obtain the full efficacy associated with an SPF, an amount of 2 mg/cm^2 of skin surface has to be applied [12]. This is a large amount but it is needed to provide a homogeneous distribution of the sunscreen, which is also very important [13, 14]. In practice, however, this amount is almost never applied for practical reasons. Investigations on the amounts of sunscreens actually applied have shown that sunscreens are applied in amounts that are lower by a factor of almost 10 than are defined in the regulations for determining the sun protection factor [15].

Another aspect to be considered in this context is that it is difficult to apply a sunscreen homogeneously to every site of the body [16]. Applying a sunscreen to one's back, for example, is hard to do correctly without assistance. In a study performed at the Center of Experimental and Applied Cutaneous Physiology, volunteers were asked to apply a sunscreen the same way as they usually would at the beach [15]. The volunteers were well aware that the topically applied sunscreen would be analyzed for the homogeneity of distribution. For these investigations, a fluorescent dye was added to the sunscreen. After application and penetration of the sunscreen, the volunteers were asked to expose themselves to the radiation emission of a party light (Woods lamp) in a dark room, making the fluorescence of the dye visible on the skin. ***Figure 2*** represents a typical image obtained from these investigations. The image clearly reveals that the users were eager to avoid any possible contact between the sunscreen and their clothes. Moreover, sunscreens were applied at a «safe distance» to the hair and eyes. An important prerequisite for avoiding such problems in the future is the development of skin physiological formulations leaving residues neither on the clothes nor on the hair and thus well accepted by the users.

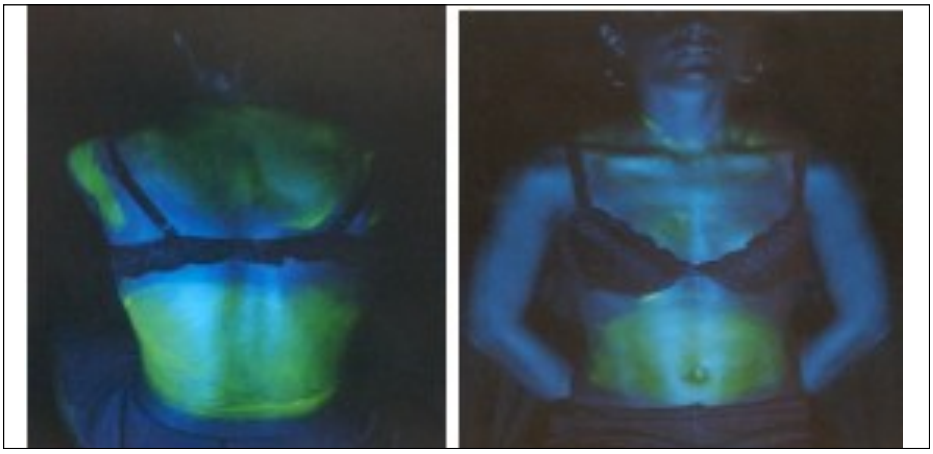

Figure 2: Images depicting sunscreen on the body surface of the volunteers following application [15]

LIGHT PROTECTION INSTEAD OF UV PROTECTION?

The solar radiation incident on the earth's surface consists of 0.5% UVB, 6.3% UVA, 39.2% VIS and 54% infrared radiation [17, 18]. Consequently, the maximum dose of solar radiation absorbed by our skin is generated in the infrared (IR) spectral range. Infrared photons are incapable of inducing free radicals directly in the skin. Nevertheless, it was shown that mitochondria exposed to infrared radiation are an essential source for the generation of reactive oxygen radicals [19, 20]. Moreover, it could be demonstrated that the gene matrixmetalloproteinase-1 (MMP-1) is upregulated [21] without a concomitant increase in the expression of its tissue-specific inhibitor TIMP-1. The resulting imbalance causes an increased breakdown of collagen fibers and ultimately leads to wrinkle formation and thus skin aging. Godly et al. could show that blue light damaged mitochondria from cultured human retinal epithelial cells [22]. Further investigations revealed that infrared A radiation not only influences just these two genes alone but that a total of 250 genes of the human skin are upregulated and 349 genes are downregulated [25] Using a mouse model, it could be shown that although infrared A irradiation did not increase the prevalence of UV-induced tumors, it essentially accelerated the growth of existing tumors [26].

Irradiation of human subjects with visible light leads to an increase in reactive oxygen species measured via chemiluminescence. In vitro exposure of epidermis models caused increased expression of matrix metalloproteinase (MMP-1) and proinflammatory cytokines [23]. In addition, Mahmoud et al. could show increased pigmentation subsequent to irradiation with visible light [24].

In 2008, Zastrow et al. published the action spectrum of the radical formation in human skin induced by solar radiation [27]. This spectrum is depicted in ***Figure 3***. It is clearly visible that the concentrations of free radicals generated in the UV are higher than in the VIS spectral range. Comparison of the total amount of free radicals induced by the complete solar spectrum reveals, however, that approximately 50% of all free radicals in our skin are induced by radiation in the VIS and IR spectral ranges. Radical production in the IR spectral range could also be shown by the depletion of carotenoids after IR irradiation, whereas different sources should provide different effects [28]. Regarding Zastrow's results we should keep in mind that there is a difference in radical formation between in vivo and ex vivo investigations, as shown by L-band EPR measurements [29]. In vivo the radicals are produced rapidly and

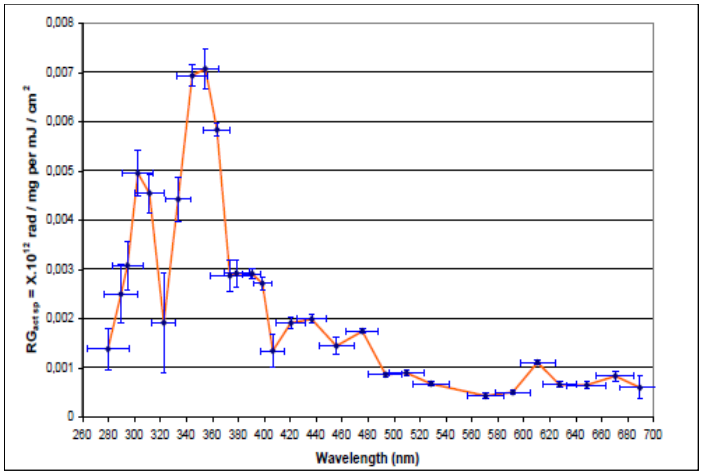

Figure 3: Action spectrum of the formation of free radicals [27]

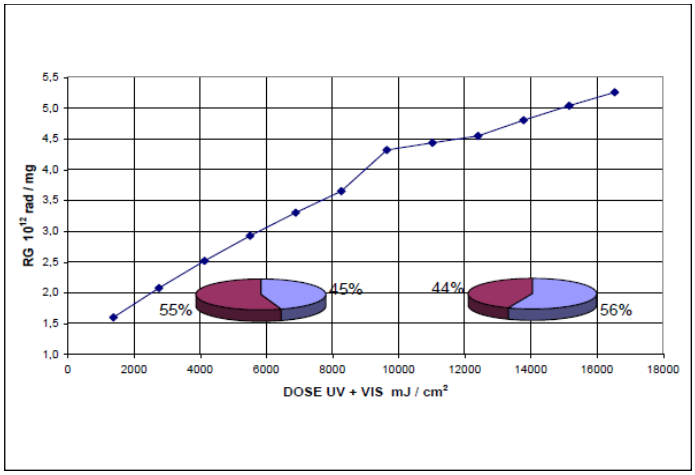

Figure 4: Free radical formation at different doses of UV+VIS radiation [31]. The two pie charts show the composition of reactive oxygen species and lipophilic radicals below the critical radical concentration of 3.5 x 10^{12} radicals per mg tissue at 6000 mJ/cm^2 and above at 14 000 mJ/cm^2

at a higher rate than shown for VIS/IR irradiation, but radical formation reached saturation. The lower radical formation ex vivo could be explained by the absence of oxygen [30].

Moreover, Zastrow et al. [31] could show that there is obviously a critical threshold for the induced free radicals. If this critical threshold is exceeded, the free radicals start damaging the skin. In general, free radicals are essential for the signaling processes in the human organism [32]. In the experiments reported by Zastrow et al., tissue samples were exposed to defined doses of UV and visible light. Subsequently, the concentrations of the induced free radicals were measured using electron paramagnetic resonance (EPR) spectroscopy. The results of these measurements are presented in ***Figure 4***. It can be seen that the amount of free radicals increases with increasing doses of UV and VIS radiation. At a radical concentration of approximately 3.5x10^{12} radicals/mg of tissue, there is a surge in the curve; radical formation clearly slows down there. Analysis of the composition of the radicals formed before and after the critical threshold shows that before the threshold the majority of the radicals formed are reactive oxygen species (ROS), whereas the radicals induced above the critical threshold are predominantly C-centered radicals, which are extremely destructive in the body. In their studies, Zastrow et al. could show that this radical composition applies not only to the UV and VIS spectral ranges, but also to the VIS and IR. Thus, the critical radical concentration represents obviously a body constant. The dose of solar light that is necessary for vitamin D synthesis is the critical radical threshold, whereas the minimal erythema dose (MED) that has been proven to cause skin damage, i.e., an erythema, exceeds this critical radical concentration considerably.

Due to the high protective efficacy of the sunscreens, people expose themselves considerably longer to direct sun radiation than when they do not protect their skin. With sunscreen application the exposure times can be extended by a factor of 3 to 10. As the protective efficacy in the UV range is very good, radical formation in this range is rare, whereas high radical concentrations, which might exceed the critical threshold, are induced in the VIS and IR ranges.

SUN PROTECTION IN THE VIS AND IR SPECTRAL RANGES

In the absence of absorbing substances that cover the complete VIS and IR ranges of the solar spectrum, sunscreens do not fully protect the skin from radical formation when it is exposed to sunlight, as absorbing, reflecting and scattering UV filter substances cannot be used for protection in the VIS and IR ranges. Therefore, increased attention should be focused on the three intrinsic protective mechanisms of the skin, and sunscreen products should be adapted to reflect these mechanisms. The first mechanism is skin thickening of the stratum corneum, i.e., the horny layer, and plays a role by absorption and scattering. As a consequence, fewer photons from solar radiation are able to penetrate into the skin. The second mechanism is melanin production, which also works by absorption and scattering. Melanosomes are good UV absorbers and exhibit also excellent scattering properties in the VIS and IR spectral ranges. Finally, there is the antioxidant protective system of the human organism including the skin, whose antioxidants are capable of neutralizing the induced free radicals before they start damaging the body [33, 34]. Free radicals are generated in the skin as a result of solar radiation and environmental hazards and they can destroy cells and cell compartments if their concentration exceeds a critical threshold. This, in turn, may result in skin aging, immunosuppression, development of skin diseases and even skin cancer.

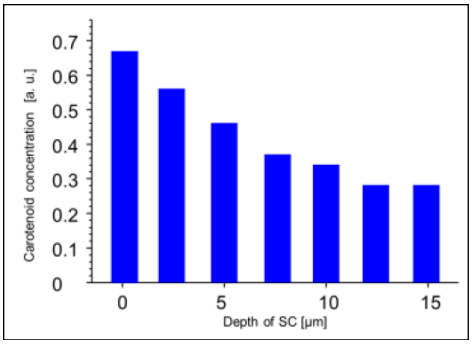

Figure 5: Distribution of carotenoids in human skin [36].

As can be seen in ***Figure 5***, the highest concentration of antioxidants is detectable on the skin surface. Typical dermal antioxidants include beta-carotene, lycopene, lutein, the vitamins A, B, E and D, polyphenols and enzymes. This high antioxidant concentration on the skin surface is plausible, as systemically applied antioxidants are ejected onto the skin surface with sweat and sebum [35, 36]. With this in mind, the antioxidant protective system of our skin is comparable to the shell of fruits and vegetables.

DETERMINATION OF THE PROTECTIVE EFFECT OF SUNSCREENS IN THE IR SPECTRAL RANGE

The protective mechanisms discussed above can also be implemented in sunscreens by incorporating titanium dioxide and zinc oxide micropigments in the sunscreen products. As these particles exhibit certain reflectance and scattering properties, they prevent certain amounts of VIS and IR radiation from penetrating into the human skin [37]. In addition, sunscreens contain antioxidants that were originally intended to stabilize the UV filters. These antioxidants provide protection also in the VIS and IR spectral ranges through neutralization of free radicals.

Radical formation in human skin can be determined in vivo or ex vivo by means of EPR spectrometry [29, 38-40]. A typical example for in vivo EPR measurements is shown in ***Figure 6***.

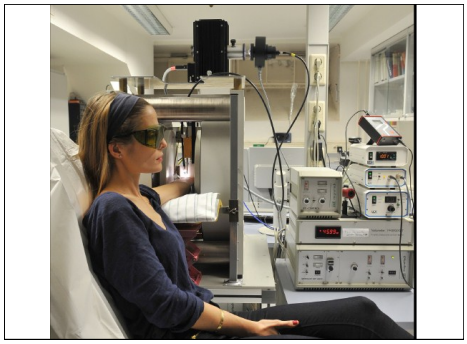

Figure 6: In vivo L-band EPR spectrometer

Based on the findings of Zastrow et al., as well as on our group's results, four different commercial sunscreens were analyzed for their protection efficacy ex vivo in the IR spectral range [37]. The four commercial sunscreen products were compared with untreated and unprotected skin samples and with the Colipa standard P3 for sunscreens containing neither pigments nor antioxidants [12]. The results of these investigations are shown in ***Figure 7.*** The magnitude of the signal is an indicator for the amount of free radicals induced in the skin by IR radiation. As shown by Meinke et al.[37], the concentration of free radicals is highest in the untreated skin. Although the results obtained for the Colipa standard are very similar to those obtained for the untreated skin, a slightly reduced radical formation was observed. This is due to the fact that the Colipa standard 3 formulation exhibits properties which smoothen the skin surface and, therefore, partly reflect solar radiation from the skin.

At the Center of Experimental and Applied Cutaneous Physiology the four commercial sunscreens were analyzed for their radical protection factor (RPF) and their optical properties [37]. The best properties were detected for Cream 4. As can be seen from ***Figure 8*** and ***Table I*** the RPF of Cream 4 is rather low. Instead, its optical properties are very high in terms of reflectance and scattering. For this product the high protective efficacy against radical formation in the IR spectral range is due predominantly to its optical properties. The situation is different with Cream 3, which ranked second. It exhibited an RPF of 119, which is considerablly higher than that of Cream 4. However, the optical properties of Cream 3 are clearly inferior, i.e., neither reflectance nor scattering are as pronounced as in the case of Cream 4. A study where the ingredients were specially composed for the study confirmed the findings [41].

	RPF
Standard	22
Cream 1	47
Cream 2	61
Cream 3	119
Cream 4	40

Table I: Radical Protection Factor (RPF) of the Formulations [37]

PROSPECTS

This article clearly indicates that sunscreens should provide protection not only in the UV range but also in the entire range of the solar spectrum. 17 Modern sunscreens should generate a pleasant sensation on the skin with well-tolerated cosmetic properties, thus encouraging consumers to apply the correct amount of the product as directed. This coincides with the experience reported from countries where people are frequently exposed to high doses of solar radiation. In these countries, people cover their skin almost completely with textiles, while parasols provide shadow. When introducing a light protection factor that will be applicable and suitable for the whole solar spectrum, the issue of sunscreen classification must be addressed. The SPF is an internationally well-established parameter for sunscreens. This parameter has been accepted by consumers and should not be changed as such. By exactly defining regulatory standards, specifying, for example, that UVA and UVB protection should be provided at a ratio of at least 1:3, it might be possible to extend the SPF coverage beyond the UVB range. In this case, the SPF should be determined in the UV spectral range as usual. For the VIS and infrared spectral ranges, however, the radical formation (RF) should be utilized to define a sunscreen's efficacy towards radical

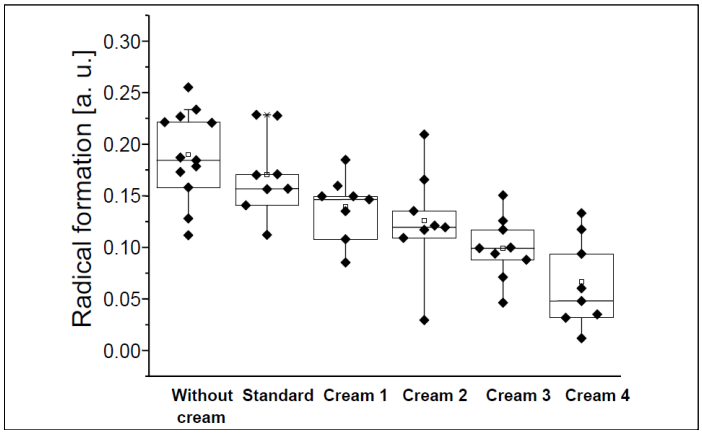

Figure 7: Radical formation in the skin due to IR irradiation (120 mW/cm^2) [37]

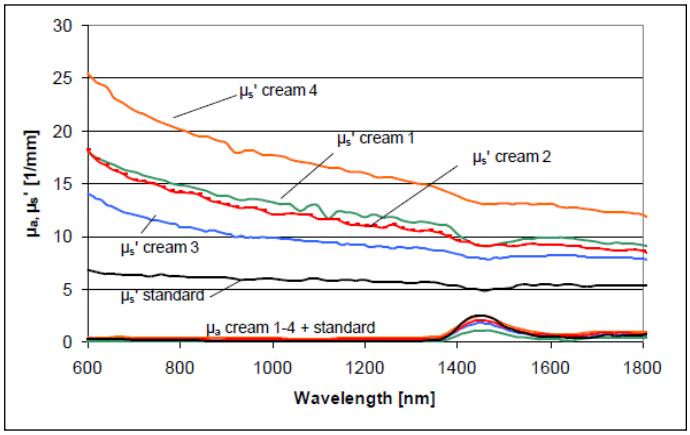

Figure 8: Absorption (μ_a) and scattering coefficient (μ_s') of the sunscreen formulations [37]

formation in these spectral ranges. Using a value yet to be determined, this RF would have to be assigned to the SPF in the UV spectral range, so that the new SPF would be a function of the currently used SPF and the RF.

Nowadays sunscreens which provide protection against radical formation in the IR spectral range are already commercially available but standardized test procedures are still missing. In the next few years, sunscreens are likely to be launched that provide protection not only in the UV but also in the VIS range. To our knowledge the protective mechanisms and determination of the protective efficacy in the VIS and IR spectral ranges should be the same.

SUMMARY

Free radicals are generated by radiation not only in the UV range but also in the VIS and IR spectral ranges of the solar spectrum. Protective mechanisms that are successfully utilized in the UV spectral range cannot be applied in the whole ranges of the solar spectrum. Therefore, the natural protective mechanism of the human body, i.e., absorption, reflectance, scattering and antioxidants, must be used in the VIS and IR spectral ranges in order to totally cover and protect the skin. Micropigments, predominantly titanium dioxide and zinc oxide, exhibit scattering and reflecting properties in sunscreens. Moreover, commercially available sunscreens contain antioxidants, which were originally intended to protect the UV filters from being destroyed. These pigments and antioxidants are effective in the VIS and IR spectral ranges. Unfortunately, pigments are added to sunscreens only to a limited extent. Normally, pigment concentrations in sunscreens do not exceed approximately 8%. The situation is quite different when it comes to antioxidants. The study performed at the CCP yielded a maximum RPF of 140 [37]. Products for medical use are currently available which exhibit an RPF of approximately 5000. There are huge development potentials in this field. In general, sunscreens produced by renowned manufacturers already provide protection in the whole range of the solar spectrum. However, the protective efficacy in the visible and infrared ranges can still be considerably improved. The measuring technologies required for this purpose are already available, but must be standardized.

ACKNOWLEDGMENT

We thank Dr. Bernd Herzog, of BASF, Grenzach-Wyhlen, Germany for the helpful discussions.

REFERENCES

[1] Zheng, Y., Chen H, Lai, W., Xu, Q., Liu, C., Wu, L., and Maibach, H.I., Cathepsin d repairing role in photodamaged skin barrier, Skin Pharmacol. Physiol., 28 (2014) 97-102.

[2] Kuchel, J.M., Barnetson, R.S., and Halliday, G.M., Ultraviolet a augments solar-simulated ultraviolet radiation-induced local suppression of recall responses in humans, The Journal of Investigative Dermatology, 118 (2002) 1032-1037.

[3] Luebberding., S., Krueger, N., and Kerscher, M., Age-related changes in male skin, Quantitative evaluation of one hundred and fifty male subjects, Skin Pharmacol Physiol., 27 (2014) 9-17.

[4] Krutmann, J., Ultraviolet a radiation -induced biological effects in human skin, Relevance for photoaging and photodermatosis, J. Dermatol. Sci., 23 Suppl 1 (2000) S22-26.

[5] Erdmann, F., Lortet-Tieulent, .J, Schuz, J., Zeeb, H., Greinert, R., Breitbart, E.W., and Bray, F., International trends in the incidence of malignant melanoma 1953 -2008--are recent generations at higher or lower risk? International Journal of Cancer Journal international du cancer, 132 (2013) 385-400.

[6] Urbach, F., The historical aspects of sunscreens, Journal of Photochemistry and Photobiology B, Biology, 64 (2001) 99-104.

[7] Fourtanier, A., Moyal, D., and Seite, S., Uva filters in sun-protection products, Regulatory and biological aspects, Photochemical & photobiological sciences , Official Journal of the European Photochemistry Association and the European Society for Photobiology, 11 (2012) 81-89.

[8] Stanfield, J.W., Ou-Yang, H., Chen, T., and Cole, C., and Appa, Y., Multi-laboratory validation of very high sun protection factor values, Photodermatology, Photoimmunology & Photomedicine, 27 (2011) 30-34.

[9] Weigmann, H.J., Lindemann, U., Antoniou, C., Tsikrikas, G.N., Stratigos, A.I., Katsambas, A., Sterry, W., and Lademann, J., Uv/vis absorbance allows rapid, accurate, and reproducible mass determination of corneocytes removed by tape stripping, Skin Pharmacology and Applied Skin Physiology, 16 (2003) 217-227.

[10] Weigmann, H.J., Schanzer, S., Teichmann, A., Durat, F., Antoniou, C., Schaefer, H., Sterry, W., and Lademann, J., Ex-vivo spectroscopic quantification of sunscreen efficacy, Proposal of a universal sun protection factor, J. Biomed.Opt., 12 (2007) 044013.

[11] Weigmann, H.J., Schanzer, S., Antoniou, C., Sterry, W., and Lademann, J., Influence of the absorption behavior of sunscreens in the short-wavelength uv range (uvb) and the long-wavelength uv range (uva) on the relation of the uvb absorption to sun protection factor, J. Biomed. Opt, 15 (2010) 055008.

[12] Colipa, International sun protection factor (spf) test method, TheEuropean Cosmetic, Toiletry and Perfumery Association, Bruxelles, 94 (1994) 289.

[13] Kluschke, F., Weigmann, H.J., Schanzer, S., Meinke M, Vergou, T., Sterry, W., and Lademann, J., Gain or loss? Sunscreen efficiency after cosmetic pretreatment of the skin, Skin Pharmacol. Physiol., 27 (2014) 82-89.

[14] Vergou, T., Patzelt, A., Schanzer, S., Meinke, M.C., Weigmann, H.J., Thiede, G., Sterry, W., Lademann, J., and Darvin, M.E., Methods for the evaluation of the protective efficacy of sunscreen products, Skin Pharmacol. Physiol., 26 (2013) 30-35.

[15] Lademann, J., Schanzer, S., Richter, H., Pelchrzim, R.V., Zastrow, L., Golz, K., and Sterry, W., Sunscreen application at the beach, Journal of Cosmetic Dermatology, 3 (2004) 62-68.

[16] Fujikake, K., Tago, S., Plasson, R., Nakazawa, R., Okano, K., Maezawa, D., Mukawa, T., Kuroda, A, and Asakura, K., Problems of in vitro spf measurements brought about by viscous fingering generated during sunscreen applications, Skin Pharmacol. Physiol., 27 (2014) 254-262.

[17] Gates, D.M., Spectral distribution of solar radiation at the earth's surface, Science, 151 (1966) 523-529.

[18] Wild, M., Gilgen, H., Roesch, A., Ohmura, A., Long, C.N., Dutton, E.G., Forgan, B., Kallis, A., Russak, V., and Tsvetkov, A., From dimming to brightening, Decadal

changes in solar radiation at earth's surface, Science, 308 (2005) 847-850.

[19] Schroeder, P., and Krutmann, J., What is needed for a sunscreen to provide complete protection, Skin Therapy Letter, 15 (2010) 4-5.

[20] Akhalaya, M.Y., Maksimov, G.V., Rubin, A.B., Lademann, J., and Darvin, M.E., Molecular action mechanisms of solar infrared radiation and heat on human skin, Ageing Research Reviews, 16C (2014) 1-11.

[21] Cho, S., Lee, M.J., Kim, M.S., Lee, S., Kim, Y.K., Lee, D.H., Lee, C.W., Cho, K.H.,and Chung, J.H., Infrared plus visible light and heat from natural sunlight participate in the expression of MMPs and type I procollagen as well as infiltration of inflammatory cell in human skin in vivo, J. Dermatol Sci., 50 (2008) 123-133.

[22] Godley, B.F., Shamsi, F.A., Liang, F.Q., Jarrett, S.G., Davies, S., and Boulton, M., Blue light induces mitochondrial DNA damage and free radical production in epithelial cells, The Journal of Biological Chemistry, 280 (2005) 21061-21066.

[23] Liebel, F., Kaur, S., Ruvolo, E., Kollias, N., and Southall, MD., Irradiation of skin with visible light induces reactive oxygen species and matrix-degrading enzymes, The Journal of Investigative Dermatology, 132 (2012) 1901-1907.

[24] Mahmoud, B.H., Hexsel, C.L., Hamzavi, I.H., and Lim, H.W., Effects of visible light on the skin, Photochemistry and Photobiology, 84 (2008) 450-462.

[25] Calles, C., Schneider, M., Macaluso, F., Benesova, T., Krutmann, J.,and Schroede,r P., Infrared a radiation influences the skin fibroblast transcriptome, Mechanisms and consequences, The Journal of Investigative Dermatology, 130 (2010) 1524-1536.

[26] Jantschitsch, C., Weichentha, M., Maeda, A., Proksch, E., Schwarz, T., and Schwarz, A., Infrared radiation does not enhance the frequency of ultraviolet radiation-induced skin tumors, but their growth behaviour in mice, Exp. Dermatol., 20 (2011) 346-350.

[27] Zastrow, L., Groth, N., Klein, F., Kockott, D., Lademann, J., Renneberg, R., and Ferrero, L., The missing link--light-induced (280-1,600 nm) free radical formation in human skin, Skin Pharmacol. Physiol., 22 (2009) 31-44.

[28] Darvin, M.E., Haag, S.F., Lademann, J., Zastrow, L., Sterry, W., and Meinke, M.C., Formation of free radicals in human skin during irradiation with infrared light, The Journal of Investigative Dermatology, 130 (2010) 629-631.

[29] Arndt, S., Haag, S.F., Kleemann, A., Lademann, J., and Meinke, M.C., Radical protection in the visible and infrared by a hyperforin-rich cream--in vivo versus ex vivo methods, Exp. Dermatol., 22 (2013) 354-357.

[30] Meinke, M.C., Muller, R., Bechtel, A., Haag, S.F., Darvin, M.E., Lohan, S.B., Ismaeel, F., and Lademann, J., Evaluation of carotenoids and reactive oxygen species (ROS) in human skin after UV-irradiation, A critical comparison between in vivo and ex vivo investigations, Exp. Dermatol. (2014) - epub.

[31] Zastrow, L., Golz K, Doucet O, Groth N, Klein F, Kockott D, and Lademann, J., Radical formation in human skin after UV/VIS-irradiation, Critical radical concentration- a new body constant? Skin Pharmacol. Physiol, 2014 submitted.

[32] Murad, F., Nitric oxide signaling, Would you believe that a simple free radical could be a second messenger, autacoid, paracrine substance, neurotransmitter, and hormone? Recent progress in Hormone Research, 53 (1998) 43-59.

[33] Lademann, J., Kocher W, Yu R, Meinke, M.C., Na Lee B, Jung S, Sterry, W., and Darvin ME, Cutaneous carotenoids, The mirror of lifestyle? Skin Pharmacol. Physiol., 27 (2014) 201.

[34] Wolfle, U., Seelinger, G., Bauer, G., Meinke, M.C., Lademann, J., and Schempp, C.M., Reactive molecule species and antioxidative mechanisms in normal skin and skin aging, Skin Pharmacol. Physiol., 27 (2014) 316-332.

[35] Thiele, J.J., Traber, M.G., and Packer, L., Depletion of human stratum corneum vitamin E, An early and sensitive in vivo marker of UV induced photo-oxidation, The Journal of Investigative Dermatology, 110 (1998) 756-761.

[36] Darvin, M.E., Fluhr, J.W., Caspers, P., van der Pool, A., Richter, H., Patzelt, A., Sterry, W., and Lademann, J., In vivo distribution of carotenoids in different anatomical locations of human skin, Comparative assessment with two different raman spectroscopy methods, Exp. Dermatol., 18 (2009) 1060-1063.

[37] Meinke, M.C., Haag SF, Schanzer, S., Groth N, Gersonde I, and Lademann, J., Radical protection by sunscreens in the infrared spectral range, Photochemistry and Photobiology, 87 (2011) 452-456.

[38] Lauer, A.C., Groth, N., Haag, S.F., Darvin, M.E., Lademann, J., and Meinke, M.C., Radical scavenging capacity in human skin before and after vitamin C uptake, An in vivo feasibility study using electron paramagnetic resonance spectroscopy, The Journal of Investigative Dermatology, 133 (2013) 1102-1104.

[39] Meinke, M.C,, Friedrich, A., Tscherch, K., Haag, S.F., Darvin, M.E., Vollert, H., Groth, N., Lademann, J., and Rohn, S., Influence of dietary carotenoids on radical scavenging capacity of the skin and skin lipids, European Journal of Pharmaceutics and Biopharmaceutics, Official Journal of Arbeitsgemeinschaft fur Pharmazeutische Verfahrenstechnik eV, 84 (2013) 365-373.

[40] Fuchs, J., Groth,N., Herrling, T., and Zimmer, G., Electron paramagnetic resonance studies on nitroxide radical 2,2,5,5-tetramethyl-4-piperidin-1-oxyl (TEMPO) redox reactions in human skin, Free Radical Biology & Medicine, 22 (1997) 967-976.

[41] Meinke, M.C., Syring, F., Schanzer, S., Haag, S.F., Graf, R., Loch, M., Gersonde, I., Groth, N., Pflucker, F., and Lademann, J., Radical protection by differently composed creams in the UV/VIS and IR spectral ranges, Photochemistry and Photobiology, 89 (2013,1079-1084.

Corresponding author
Juergen.lademann@charite.de

IFSCC INTERNATIONAL FEDERATION OF SOCIETIES OF COSMETIC CHEMISTS

Multicenter Study on the Effect of Various Test Parameters on the Curl Retention Results of Hairsprays

U. Aßmus (Emil Kiessling GmbH), S. Bielfeldt (proDERM Institute of Applied Dermatological Research), H.-M. Haake (BASF Personal Care and Nutrition GmbH), H. Hensen, P. Hössel (BASF SE), G. Lang, H. Leidreiter (Evonik Industries AG (Care Specialties)), A. Markowetz (Procter & Gamble Service GmbH), V. Martin, B. Nöcker (KAO Germany GmbH), M. Pfaffernoschke (AkzoNobel Surface Chemistry AB), E. Poppe (Henkel AG & Co. KGaA), H. Schmidt-Lewerkühne, A. Schwan-Jonczyk, J. Wood (KAO Germany GmbH), F.-J. Wortmann (University of Manchester)

The Working Group for "Hair Treatments" from the DGK (German Society for Scientific and Applied Cosmetics).

Keywords: Hairspray, curl retention test, weather resistance, multicenter study, ring study

ABSTRACT

In the development of hairspray formulations, great emphasis is placed on the selection and composition of setting polymers, as complex effects have to be taken into consideration and the expectations of consumers fulfilled. An essential part of consumer acceptance is the hold (setting ability) and the durability of hold over a longer period, especially under particular environmental conditions. As setting polymers absorb moisture from the atmosphere to a greater or lesser degree depending on their hydrophilic properties, durable hold and resistance to weather conditions can vary. The well-publicized curl retention test is one way of testing resistance to weather conditions in the product development phase. The Working Group for "Hair Treatments" from the DGK (German Society for Scientific and Applied Cosmetics) carried out a multicenter study in six test centers to examine the effect of various parameters on the results of the curl retention test. It was shown that through the standardization of influential parameters such as rollers, winding of the curl, spraying time, spraying distance, spraying method, humidity and temperature, the effect of the test centers was minimized and a significant differentiation between different hairspray formulations with different setting polymers was achieved.

INTRODUCTION

When developing hair styling products the mechanical properties and interaction between the hair and the polymer film former play an important role in consumer acceptance, especially with regard to hold (setting ability) and the durability of hold. There are a wide range of film formers and hydrophilic polymers available, which are water soluble to a greater or lesser degree, that can achieve the hold and durability of hold desired for different product types. These are used in styling products either individually or in combination with each other and can be easily removed from the hair in one hair wash.

However, hydrophilic polymers have one disadvantage. Depending on the strength of the hydrophilic property of the polymer, they absorb water from the atmosphere to a greater or lesser extent, thus partly or entirely losing hold. The stronger the hydrophilic tendency, the more water is absorbed and the lower the durability of hold.

In scientific literature curl retention (the behavior of curls in high humidity conditions) is frequently described as a measure of the lastingness of the hold of hair styling products and polymer films ([1] – [8]).

A curl retention measurement describes the behavior of a defined hair curl that has been treated with a hair styling product. To do this a curl is formed into a water wave of defined shape, dried and then treated with a styling product. Herein lies the first problem, how to exactly quantify the amount of product that is applied to the hair. The treated and dried curl is then hung up and exposed to various climatic conditions. The length of the hanging curl is measured over time. The slower the lengthening of the curl is, the better the curl retention.

The methodological details and parameters are often not described sufficiently in the scientific literature, with industrial test laboratories and independent research institutes carrying out these types of tests using their own individual methods. This leads to results that cannot be compared with each other.

The Working Group for "Hair Treatments" from the DGK (German Society for Scientific and Applied Cosmetics) set out to analyze the effect of various test parameters on curl retention in a thorough and comparative multicenter study using hairsprays as an example.

EXPERIMENTAL

Six test centers from industry and laboratory service providers took part in the study.

Structure of the study and test procedure

In the first part of the study three hairsprays containing either 3% PVP/VA Copolymer, 3% VA/Crotonates/Vinyl Neodecanoate Copolymer or 3% Acrylates Copolymer were tested and compared with each other with regard to their curl retention. Each test center carried out the tests following their own methodology but where the following parameters should to be kept as uniform as possible: hair type (Caucasian, virgin/untreated), hair quantity (weight, original length), binding of the hair tress (flat tress, round wound tress), presetting method for the curl (water wave), application conditions (spray distance) and the evaluation.

The experimental variables were the method of application (immersing, spraying, static or dynamic application), shape of the roller (tube or spiral, number of winds per tress), how tight the tress was wound (with or without added weight), diameter of the roller, application quantity, drying conditions (length of time, temperature, humidity), hanging conditions (temperature, humidity, with or without added weight) and evaluation of the curl while hanging (visual, physical).

In accordance with the test centers' previous experience the following parameters were identified as having a significant effect on the test results: preparation of the hair tresses (pre-test damage, pre-test washing), geometry of the tress (flat, round), conditions while the tress is hanging (speed of the air circulation, fan), material of the roller (PMMA, Teflon) as well as the evaluation methods

(control length of the tresses, calculation formula, curl length at time 0).

The formulation to be tested was applied to the wound hair tress; the tress was then dried and carefully removed from the roller making sure that the polymer film was not broken or damaged. Damage to the film can affect the results of curl retention tests significantly as there can be a loss of the curl retention effect of the polymer at these breakage points. Furthermore, stronger water absorption can also occur at these points causing the curl to relax more strongly and faster.

An untreated curl formed with a water wave was used as a control.

The curls set with the test products and the control water wave curl were then hung up and exposed to constant climate conditions with respect to temperature and humidity. The lengthening of the curls was measured at different predefined time intervals.

The curl retention [CR] was calculated using the following formula:

$$CR\ [\%] = (L_0 - L_t) * 100 / L_0 - L_{start})$$

L_0 = original straight length of the tress
L_t = length of curl at time t
L_{start} = starting length of the curl

The results were presented showing the measurements over time.

The first part of the multicenter study showed differences between the curl retention of the three hairspray formulations and the water wave. However, the results varied greatly among the test centers (***Figure 1***).

The results did not show any satisfactory distinction between the three polymers or between the polymers and the water wave (***Figure 2***). The water wave was not included in the test in three of the test centers.

Furthermore, despite the planned standardization of various parameters there were big differences in the methods used in the individual test centers. There were significant differences, for example, in the weight and length of the hair tresses used. Other factors also had a considerable effect on the results in the different centers, such as the shape and material of the rollers used (spiral rollers made of Teflon with a defined twist, smooth PMMA rods, commercially available spiral rollers) or the quantity and method of applying the test substance to the hair (as a hair spray or dipping in the polymer solution). These differences led to the decision to use spiral rollers with a defined diameter and twist and to spray the curl while it is still on the roller with an aerosol in the next series of tests. The use of spiral rollers leads to a more uniform curl shape and thus a more uniform starting value than with rod rollers. Although the latter allow a tighter winding of the hair, this leads to greater variation in the number of curves in the curl. Spraying the test substance in aerosol form instead of dipping in a polymer solution has greater practice relevance and also leads to better results.

In preparation for the second stage of the multicenter study, standardized instructions were developed for the test centers based on observations from the first phase in order to standardize as many parameters as possible.

The following conditions and parameters were fixed:

Hair tresses:

Weight:	1 g
Width:	1 cm
Tress geometry:	round
Tress type:	glued tress
Total length:	20 cm
Length of hanging hair:	17 cm
Number:	4
Level of damage:	undamaged
Supplier:	Kerling, Backnang

Preparation of the tresses:

The hair tresses were washed twice by hand with a 14% sodium laureth sulfate solution under running tap water at a temperature of 38°C ± 1°C in order to remove any surface impurities or static. First the tresses were wet fully with tap water, then 1 g of 14% sodium laureth sulfate solution was massaged and lathered into the hair for one minute, and finally the hair was rinsed under running water for one minute. This procedure was carried out twice. The tresses were then wound around the standard roller (see below) while damp.

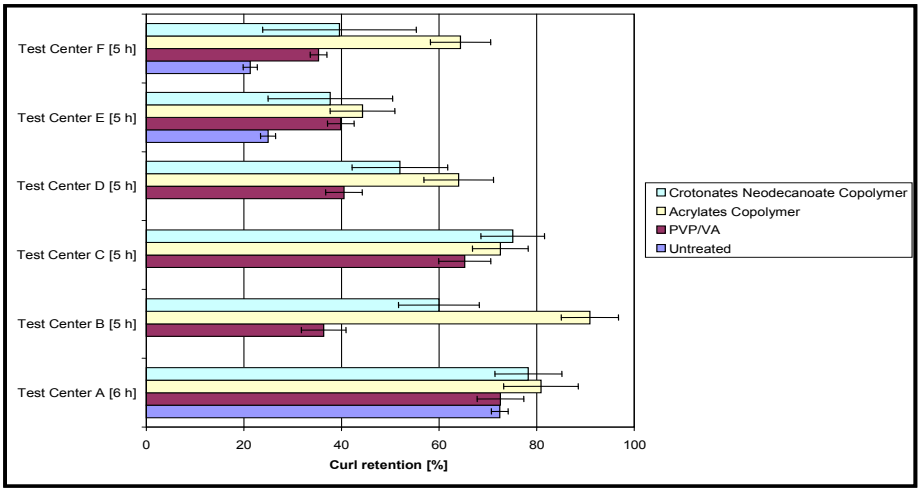

Figure 1: Curl retention – results according to test centers

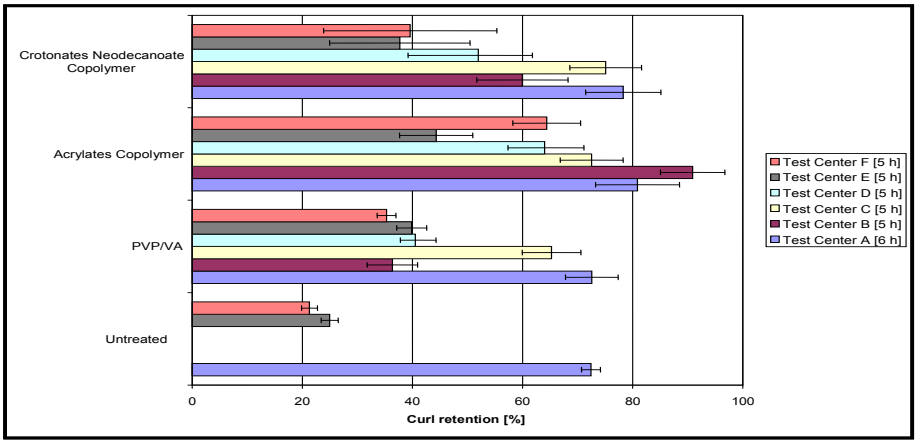

Figure 2: Curl retention – results according to test formulation

Rollers

Each test center was supplied with standard rollers:

Type: spiral rollers (***Figure 3***)
Material: Teflon
Diameter: 12 mm

The tresses were wound around the rollers using a weight of 10 g (equivalent to about 98 mN) in order to create uniform tension.

When winding the hair around the rollers it was recommended to use a construction whereby the roller was hung at an angle enabling the hair tress to be wound at right angles to the groove. The weight was attached to the end of the hair tress. This allowed the tress to be wound flat, directly into the groove of the roller. The ends were secured to the roller with a small clip, making sure that the ends were distributed smoothly and evenly in the groove of the roller (***Figure 4***). Finally, the weight was removed from the end of the wound hair tress.

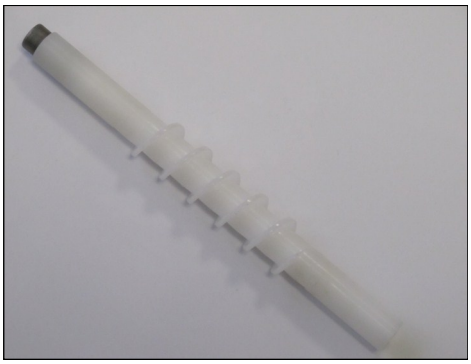

Figure 3: Teflon roller

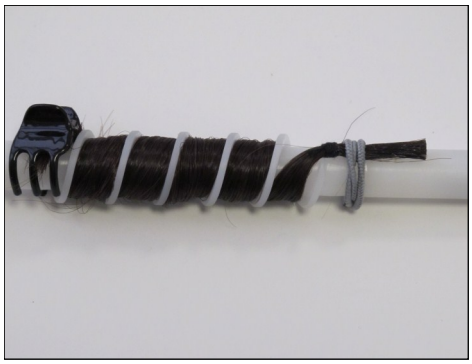

Figure 4: Teflon roller with hair tress wound around it

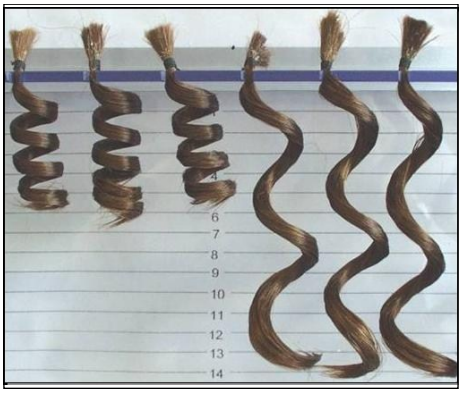

Figure 5: Example of curls hanging in a climate chamber (left: original state when hung; right: after 24 hours)

Test formulation:

The following two polymers were selected for the hair spray test formulations as, due to their chemical and physical properties, a clear difference between them and between them and the water wave was to be expected.

3% PVP/VA copolymer
brand name: Luviskol™ VA 37 I (PVP/VA)
supplier: BASF

3% Octylacrylamide/acrylates/
butylaminoethyl methacrylate copolymer
brand name Amphomer™ (OABAM)
supplier: Akzo Nobel

Where necessary the polymer was neutralized using amino methyl propanol (AMP). The polymers were then dissolved in 60% ethanol and put into aerosol cans with 40% diethyl ether.

Application

The application of the hair sprays was carried out under the following conditions:

Spraying time: 3 s and 5 s
Spraying distance: 25 cm

The hair spray was applied to the wound hair while the roller was rotated at a constant speed of 160 r/min. An up and down movement of the aerosol or the roller during spraying was not required.

Water wave

Untreated hair tresses, which were also wound onto rollers while damp using a 10 g weight for uniform tension, were used as a control.

Hanging the curls in the climate chamber

An apparatus in which the curls are fixed perpendicularly (***Figure 5***) proved to be the best option for hanging the curls in the climate chamber.

Climate conditions

The treated curls were dried while still wound on the rollers, first for 1 hour at 35°C, followed by a conditioning period of 18 hours at 22°C and 55% relative humidity.

After the conditioning period the curls were carefully removed from the spiral rollers without breaking the polymer film.

The following test conditions for hanging the tresses were selected:

Temperature: 21°C and 25°C
Relative humidity: 75% and 90%

Calibration of the humidity in the climate chamber for conditioning and hanging the curls was carried out using a capacity humidity sensor, which was supplied to each test center. Thus uniform climate conditions could be guaranteed in all test centers.

Lengthening of the curls was measured visually (parallax free) or physically using a laser after 0, 0.5, 1, 2, 3, 5 and 8 hours.

RESULTS

It can be seen in ***Figures 6 + 7*** that under the chosen conditions it is possible to show a greater differentiation between the products at 75% relative humidity and 5 seconds spraying time than at 90% relative humidity. There was no difference between the water wave and the PVP/VA copolymer at 90% relative humidity.

Analysis of the results

All of the parameters were subjected to multiple regression analysis using Cornerstone software. Due to the complex nature of the data, simple relationships between system variables were identified and their effect on the results investigated.

For the purpose of the evaluation the following variables were selected:

Predictable values (predictor)

- Test center (TC)
- Hair spray formulation (HS)
- Spraying time (ST)
- Relative humidity (RH)

Target values (response)

- Curl retention in % at different observation times 0 - 8 hours (CR0, CR 0,5, CR1 ... CR8)
- Curve torsion value Tau
- Equilibrium curve value S_{inf}

Effect of the test centers

It was found that, despite standardization of the test conditions, the biggest effect came from the individual test centers, whereby one of the test centers deviated significantly from the rest and proved to be a statistical outlier (***Figure 10***).

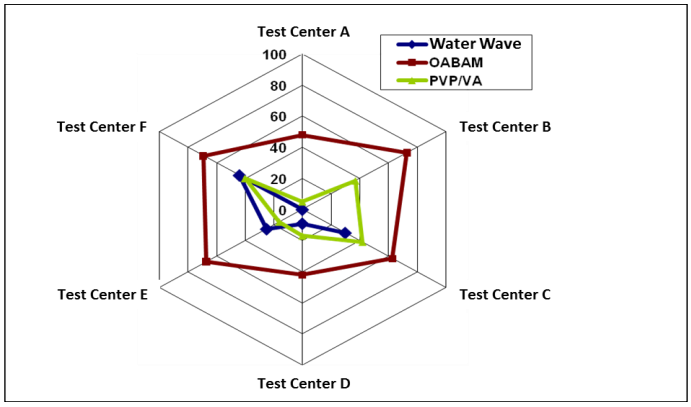

Figure 6: Curl retention results with 5 s spraying time and measurement after 5 h at 90% relative humidity

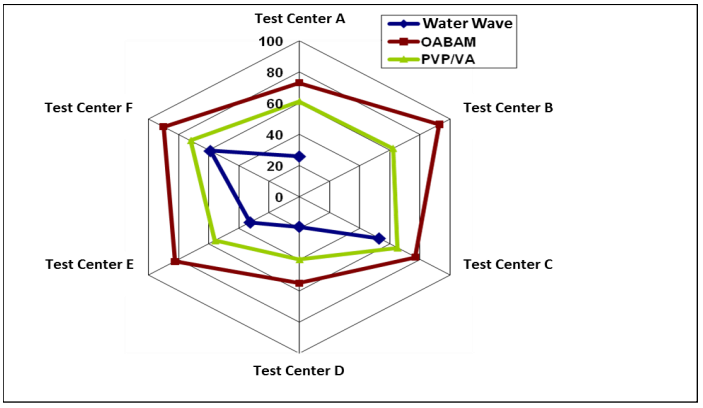

Figure 7: Curl retention results with 5 s spraying time and measurement after 5 h at 75% relative humidity

Removal of the results from Test Center D led to an improved and more uniform picture in the adjusted response graph (***Figure 11***). It was found that in this laboratory the hair tresses were hung at a slight angle and did not hang perpendicularly in the climate chamber; this led to measurement of shorter original hanging lengths of the curls than in the other test centers. In this test center it was still possible to differentiate between the two polymers and the water wave.

As a result of the tress being fixed incorrectly to the roller (***Figure 9***) the curl hung at an angle in the climate chamber and led to significantly deviant values in the course of curl relaxation. Consistent results could only be achieved in the ring study (***Figure 10 + 11***) when the curl was fixed correctly (***Figure 8***).

In order to make the effect of the individual parameters on the results of the curl retention tests clearer and highlight errors or erroneous interpretations, the results are presented both before and after elimination of the outlier data.

Effects before outlier elimination

Effect of the observation time

The analysis before the outlier was detected showed that the measurement times of the curls after 30 minutes and 1 hour were not suitable for the evaluation. The effect of the test centers was as high as the effect of the test formulation (***Figure 12***).

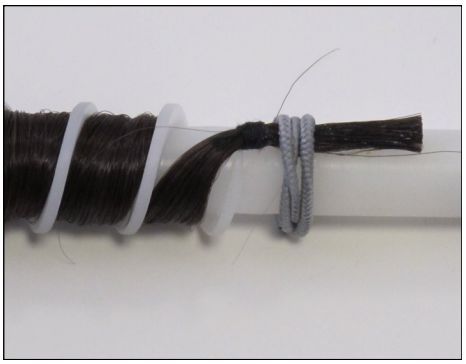

Figure 8: Curl fixed correctly

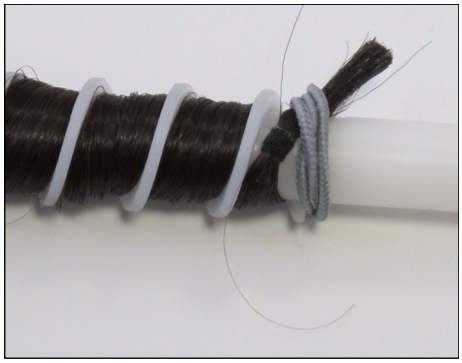

Figure 9: Curl fixed incorrectly

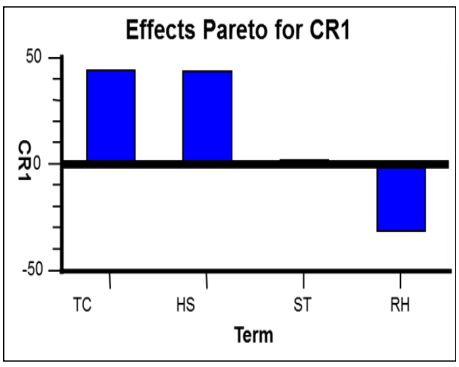

Figure 12: Effects at one measurement time - after the curls had hung for 1 hour

Effect of spraying time and humidity

The multiple regression provided by the Cornerstone™ Software showed that the spraying time had no effect on the values at any of the measuring times (***Figure 13***).

The best differentiation between the two test hair spray formulations and the water wave was achieved at 75% relative humidity and 5 seconds spraying time (***Figure 14***).

In comparison, measurements made at 90% relative humidity with 5 seconds spraying time show no satisfactory differentiation between the test hair spray with PVP/VA and the water wave (***Figure 15***), which can be explained by the high absorption of water from the atmosphere by the polymer PVP/VA. Relaxation of the curls treated with PVP/VA was comparable with that of the water wave.

Effect of the curve torsion and equilibrium constants

In order to evaluate the relaxation curve (***Figure 16***) a functional adjustment was carried out in which the exponential decrease was viewed in relation to the equilibrium constant:

$$\text{Curl retention [\%]} = S_{inf} + \Delta S^{(-t/tau)}$$

S_{inf} = Equilibrium constant (CR-infinite)
Tau = Parameter of the falling curve (curve torsion)
ΔS = 100% - curl retention at time 't'
t = Observation time

When analyzing the data the effect of the test centers was found to be greater than that of the hair spray formulation; therefore this parameter was deemed to be unsuitable .

In contrast to this, the effect of the test centers on the equilibrium constant Sinf is significantly less than that of the hair spray formulation (***Figure 18***).

Effects of outlier elimination

After eliminating the outlier laboratory the observation times 1 (CR1), 3 (CR3), 5 (CR5)

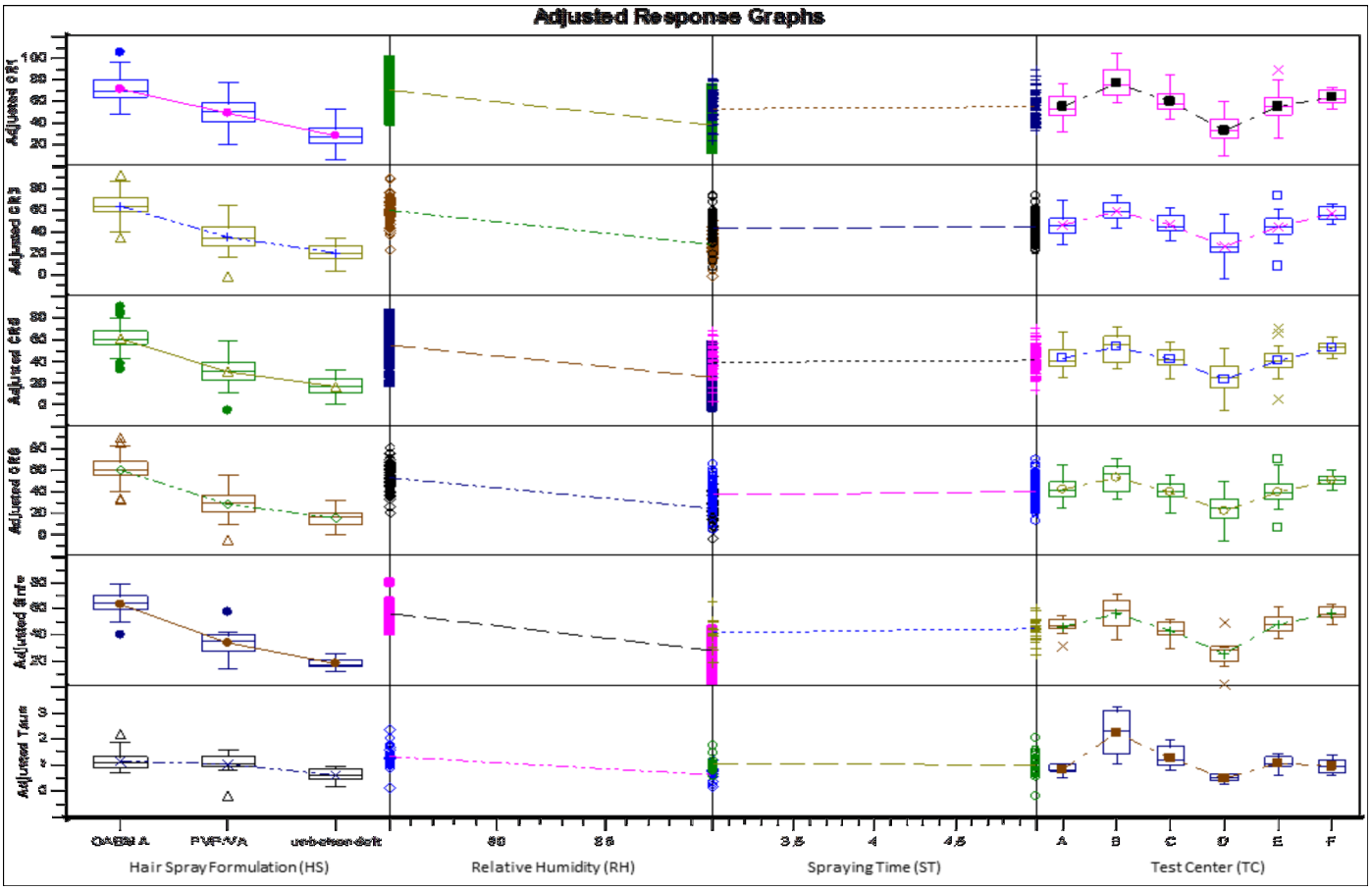

Figure 10: Adjusted response graph before elimination of outlier values for all data

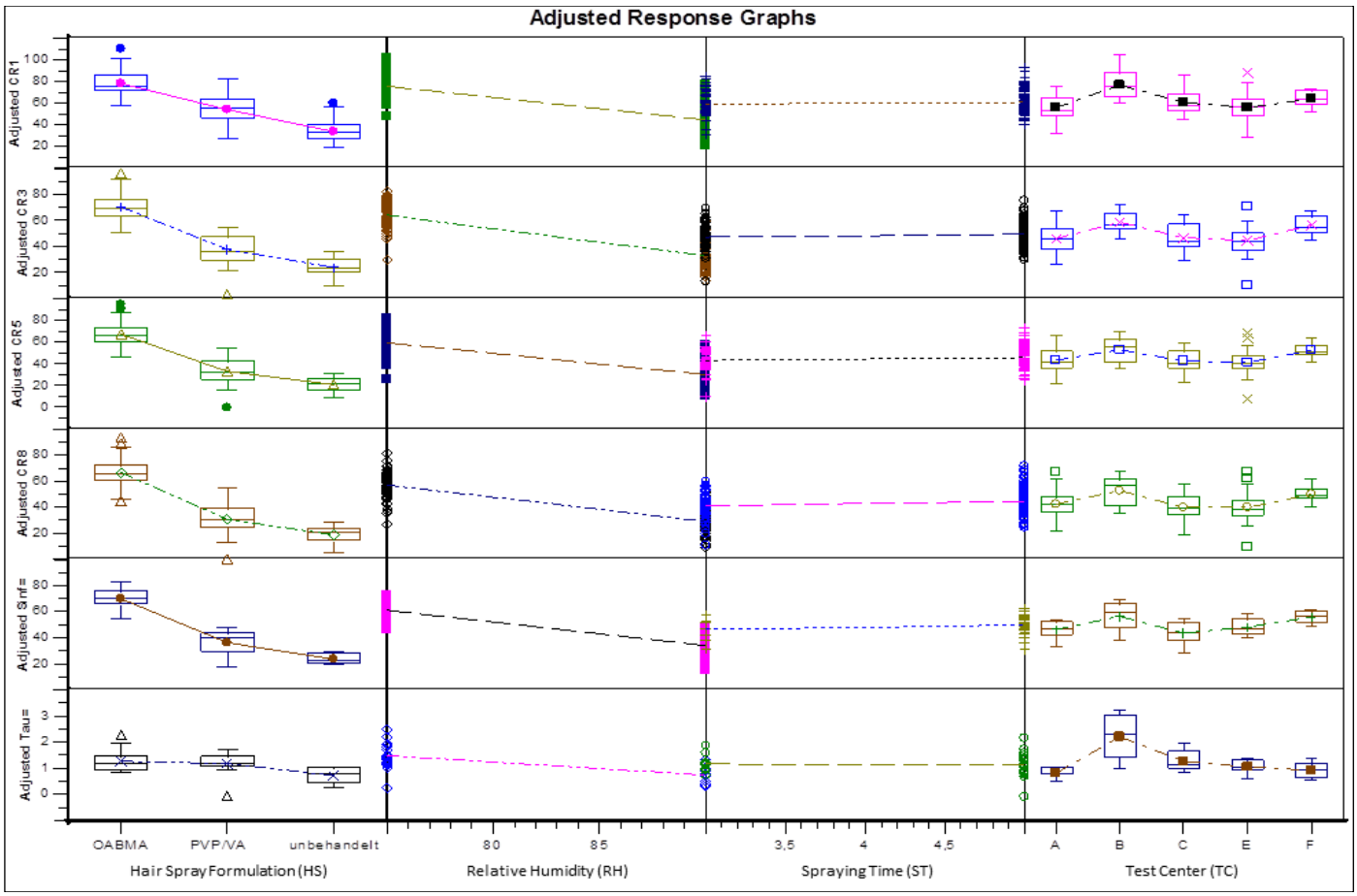

Figure 11: Adjusted response graph after the elimination of outlier values for all data (i.e. without data from test center D)

and 8 hours (CR8) as well as the equilibrium constant Sinf could be used for the evaluation of the differences between hair spray formulations. In all cases the effect of the test centers was considerably less than that of the hair spray formulation (***Figure 19***).

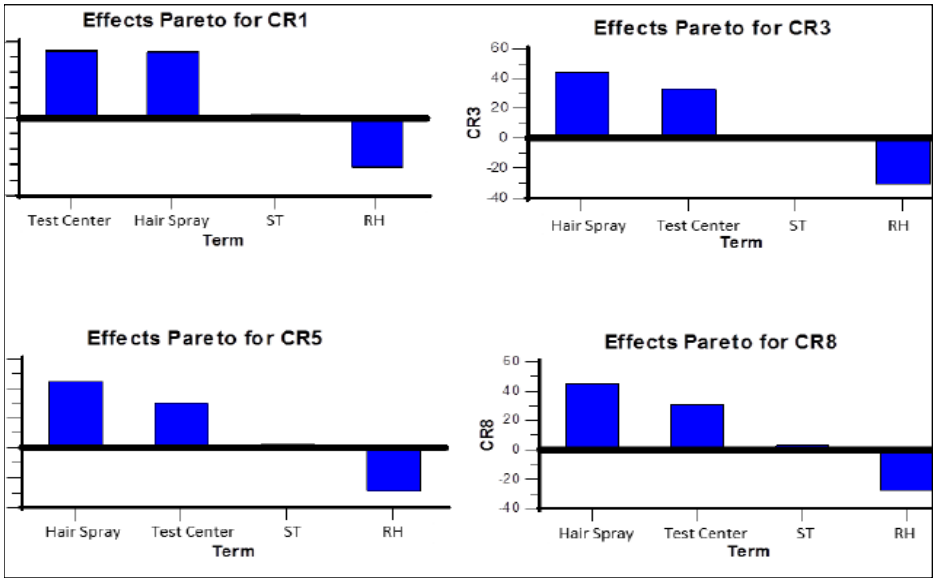

Figure 13: Evaluation of the effect of the spraying time after 1, 3, 5 and 8 hours

CONCLUSIONS

With this multicenter study the DGK Working Group was able to demonstrate the most important influential parameters on curl retention using hair sprays as an example.

By standardizing the methods used, effects on the results due to such factors as hair tresses, rollers, winding methods, humidity and application of the product were minimized and possible errors highlighted.

Under the chosen conditions it was possible to detect differences in relaxation of the curls in high humidity conditions between those treated with the hair sprays with PVP/VA or Octylacrylamide/Acrylates/ Butylaminoethyl Methacrylate Copolymer, with the water wave as a base value.

The best differentiation was achieved under the following conditions: 22°C, 75% relative humidity, 5 seconds spraying time and 25 cm spraying distance. To achieve uniform tension of the curl on the roller, a weight of 10 g was used to wind the tress onto a spiral roller made of Teflon.

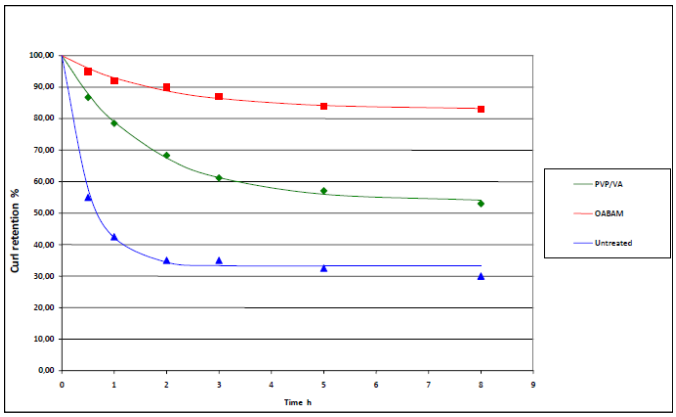

Figure 14: Differentiation between the polymers and the water wave at 75% relative humidity and 5 seconds spraying time (typical data)

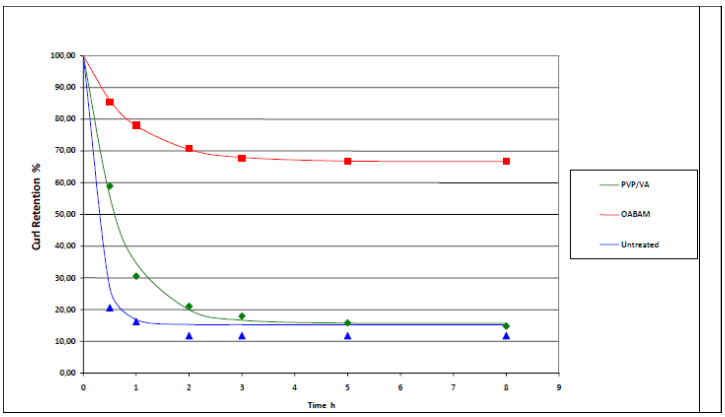

Figure 15: Differentiation between the polymers and the water wave at 90% relative humidity and 5 seconds spraying time (typical data)

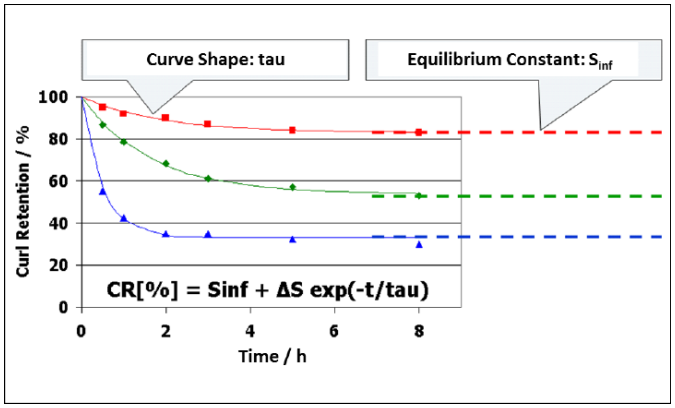

Figure 16: Curve torsion and equilibrium constants at 75% relative humidity and 5 seconds spraying time

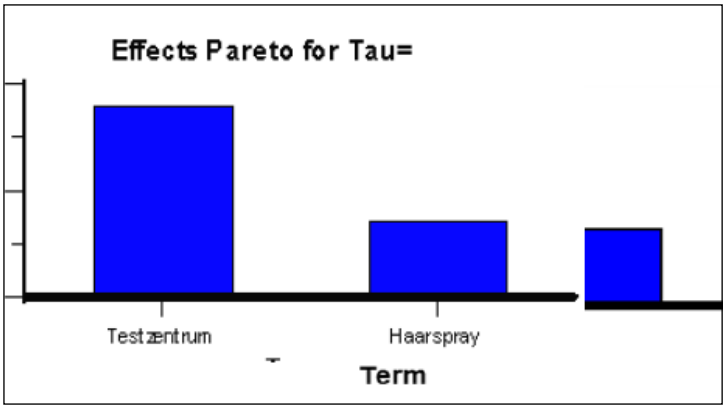

Figure 17: Evaluation of the curve torsion Tau

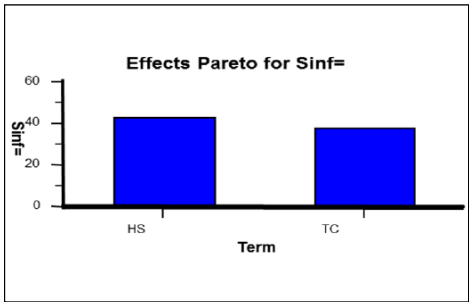

Figure 18: Analysis of the equilibrium constant Sinf

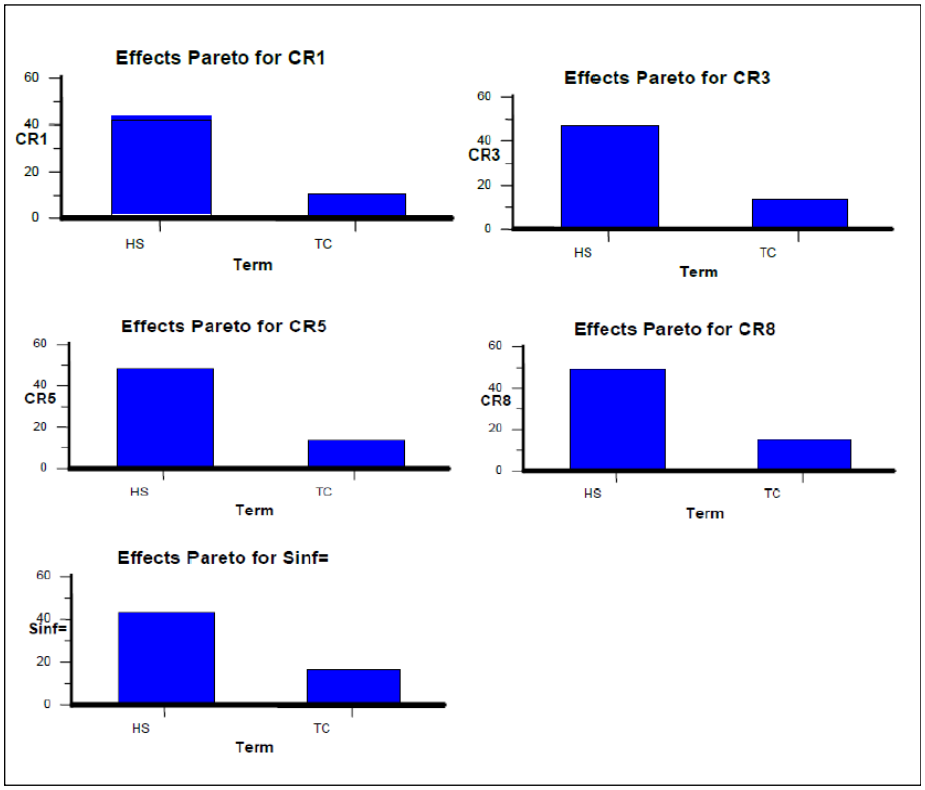

Figure 19: Evaluation of the observation times 1, 3 , 5, 8 hours and Sinf

ACKNOWLEDGEMENTS

We would like to thank everyone who worked on the execution and evaluation of this study in the various test centers.

REFERENCES

(1) Micchelli, A.L., Koehler, F.T., Polymer Properties Influencing Curl Retention at High Humidity, J. Soc. Cosm. Chemists, ***19*** *(1968), 863 – 880.*

(2) Berkhout, H., Hairspray Part 1 - Trocknungszeiten und Curl Retention von Produkten des europäischen Marktes, Aerosol Spray Report, ***32*** *(1) (1993), 28 – 40.*

(3) Berkhout, H., Hairspray Part 2 - Trocknungszeiten und Curl Retention von Labormustern, Aerosol Spray Report, ***32*** *(2) (1993), 71 – 78.*

(4) Berkhout, H., Hairspray Part 4 - Einfluß des Neutralisationsgrades und der Beigabe anderer chemischer Substanzen auf die Curl Retention und Curl Droop, Aerosol Spray Report, ***32*** *(3) (1993), 122 – 128.*

(5) Robbins, C.R., Chemical and Physical Behaviour of Human Hair, Springer Verlag, New York, 1994, 3rd Edition, p. 352.

(6) Marlier, L., Selter, M., Bimodal Polymers for Next Generation Hair Styling Products, SÖFW-Journal, ***130*** *(2004), 61 – 68.*

(7) Hössel, P., Pierobon, M., Wood, C., Polyquaternium-68, SÖFW-Journal, ***131*** *(2005), 19 – 29.*

(8) Krzysik, D., Rafferty, D.W., Tamarselvy, K., Zellia, J., Liu, X., Shlepr, J,: A Stiff-Hold Styling Polymer with Humidity Resistance, Happi Magazine, ***4*** *(2007), 89 – 95.*

Corresponding author
email: jonathan.wood@kao.com